ANALYSIS OF ACTIVE CONTROL OF

CANTILEVER BEAM BENDING VIBRATIONS

THESIS

AFIT/GA/AA/78D-6   Donald T. Palac
                     2Lt   USAF

ANALYSIS OF ACTIVE CONTROL

OF CANTILEVER BEAM BENDING VIBRATIONS,

THESIS

Presented to the Faculty of the School of Engineering

of the Air Force Institute of Technology

Air University (ATC)

in Partial Fulfillment of the

Requirements for the Degree of

Master of Science

by

Donald T. Palac

2Lt   USAF

Graduate Astronautical Engineering

December 1978

PREFACE

I am indebted to several people for the help and support they provided during the long haul towards this finished product. Dr. Robert A. Calico, my advisor, was a source of encouragement as well as technical guidance. Capt. James Silverthorn helped me unravel the tangled knots of optimal control theory. I would like to thank Capt. John B. Hungerford for his understanding. Finally, I am grateful to my typist, Mary Dunnebacke, whose friendship contributed to more of this thesis than just the typed pages.

CONTENTS

LIST OF FIGURES

ABSTRACT

Active control of bending vibrations in a cantilever beam is examined using a digital computer model of beam and controller. The controller uses the discretized beam equation of motion in a linear control system, which uses a Luenberger observer to reconstruct modal amplitudes and velocities from the sensor output. Feedback gains obtained from a steady state optimal regulator drive a force actuator. The model is used to examine three areas of active control of bending vibrations. First, impact on control effectiveness is investigated for iterative changes in elements of the state weighting matrix, part of the quadratic performance index minimized for the steady state optimal regulator. Second, the steady state optimal regulator is replaced with classical control through addition of open loop zeroes to the system transfer function. Third, the sensor model is changed to include position and rate information and rate information only. State weighting matrix element changes selectively produce increased damping of the mode associated with the changed element. Breakdown of the observer model, and instability, occurs when the change in an element exceeds a limit peculiar to that element and its relative magnitude. Control through classical feedback compensation is at least as effective as optimal control by the steady state optimal regulator. Addition of rate information to the sensor model causes instability because of numerical inaccuracies in the solution of the linear equation producing the Luenberger observer state estimation.

INTRODUCTION

Increasing interest in construction of large space structures such as solar energy collectors and large orbiting radio telescopes, present unprecedented problems in flexible satellite attitude control. Separation of control and structural frequency bandwidths to control undesirable structural vibrations may not be possible for these large space vehicles. Active controllers applied to structural vibrations may provide an answer.

Balas (Ref 1) described a method for applying active control to a simply supported beam. The equation of motion of the beam in bending is discretized by the normal modes approximation. This information is incorporated in a linear control system, where information from the sensor is used to estimate the modal amplitudes and velocities through a Luenberger observer. The steady state optimal regulator produces control proportional to the modal amplitudes and velocities by minimizing a performance index. This control is applied to the beam by a force actuator.

Hungerford (Ref 4) implemented Balas' method in a digital computer model of a cantilever beam. He showed that, at least within the limits of his investigation, the method of control appeared feasible for controlling bending vibrations in a cantilever beam. Hungerford looked at the influence of control weighting, sensor and actuator location, and observer error on control effectiveness. In this thesis, the influence of state weighting changes, different sensor models, and the

application of classical control techniques are investigated.

The steady state optimal regulator applied to a finite number of states in a beam provides incomplete control; that is, an infinite number of states remain uncontrolled by the regulator regardless of the number of states controlled. For such a system, there is a need for determining the effects of changing the weighting in the quadratic performance index, which is minimized to produce the "optimal" regulator. Hungerford investigated the effect of changing the control weighting matrix on the control effectiveness. The first purpose of this thesis was to complete the study of the effect of weighting changes by determining the effect of state weighting matrix element changes on the effectiveness of control.

During the study of the optimal regulator, the root locus indicated the effects of weighting changes. Examination of several root locus diagrams suggested the application of classical control techniques. By placing zeroes at selected points on the root locus, it was expected that effective control might be acheived. Examination of simple feedback compensation applied to a vibrating beam became a second purpose for this thesis.

The Luenberger observer in Hungerford's study used input from a position sensor. Foreseeing application to physical systems, some alternatives in selection of sensors is desirable. The third purpose of this thesis was to expand Hungerford's study to include a rate sensor and a position-rate sensor.

From a starting point offered by Balas, Hungerford began an investigation of the active control of bending vibrations

in a cantilever beam. The overall purpose of this thesis was to further that investigation. The specific areas examined were: the effect of changing elements of the state weighting matrix; the application of simple feedback compensation; and the use of rate and position-rate sensors.

ANALYTIC TECHNIQUES

The basic vehicle for most of the investigation was a digital computer model of a cantilever beam, Luenberger observer, and optimal regulator developed by Hungerford.

For the investigation of state weighting changes and different sensor types, control was applied to the first two normal modes of bending vibration, with a third mode included as a residual mode. This simplified the study without loss of generality, and assured compatability with the "Total" program, developed by Larimer (Ref 5) for control systems analysis and design. "Total" was used to generate root locus diagrams from the linear system matrices produced by the Hungerford's linear system model.

Hungerford's computer model of the system is based on the following block diagram:
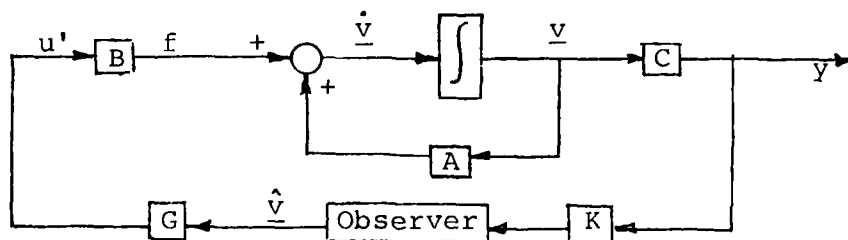
$$
\begin{aligned}
v &= \text{state vector} \\
\hat{v} &= \text{estimated state vector} \\
[A] &= \text{coefficients from discretized beam equation} \\
\{B\} &= \text{control coefficients matrix} \\
\{C\} &= \text{output coefficients matrix} \\
\{G\} &= \text{feedback gain matrix} \\
\{K\} &= \text{observer gain matrix} \\
u' &= \text{control input} \\
f &= \text{control force signal}
\end{aligned}
$$

In order to form the state equations we consider the equation of motion for a cantilever beam with no applied

-4-

external forces:

$$-EI \; \frac{\partial^4 y(x,t)}{\partial x^4} \; = \; m \; \frac{\partial^2 y(x,t)}{\partial t^2} \tag{1}$$

where the stiffness, EI, and the mass per unit length, m, are
constant along the beam length. The equation is discretized
by using a normal mode approach where:

$$y(x,t) \; = \; \sum_{i=1}^{n} \; \phi_i(x) \underline{u}_i(t) \tag{2}$$

The normal modes $\phi_i(x)$ are found by solution of the special por-
tion of eq 1, and they represent the mode shapes. The modal
amplitudes $\underline{u}_i(t)$ form the basis of the linear system model.

The linear system is constructed on a state vector $\underline{z}$
where:

$$\underline{z} \; = \; \left\{ \underline{v}_c{}^T \; \vdots \; \underline{e}^T \; \vdots \; \underline{v}_r{}^T \right\}^T$$

$$\underline{v}_c \; = \; \left\{ \underline{u}_i{}^T(t) \; \vdots \; \underline{u}_i{}^T(t) \right\}^T \qquad i=1,2$$

$$\tag{3}$$

$$\underline{v}_r \; = \; \left\{ \underline{u}_i{}^T(t) \; \vdots \; \underline{u}_i{}^T(t) \right\}^T \qquad i=3$$

$$\underline{e} \; = \; \left\{ \hat{\underline{v}}_c - \underline{v}_c \right\}$$

The subscripts c and r refer to the controlled and residual
modes, respectively. The linear system representing the
cantilever beam, Luenberger observer, and steady state optimal
regulator has the form:

$$\dot{z} = \begin{bmatrix} [A_c] + \{B_c\}\{G\} & \vdots & \{B_c\}\{G\} & \vdots & \{0\} \\ \hline \{0\} & \vdots & [A_c] - \{K\}\{C_c\} & \vdots & \{K\}\{C_r\} \\ \hline \{B_r\}\{G\} & \vdots & \{B_r\}\{G\} & \vdots & [A_r] \end{bmatrix} z \qquad (4)$$

The subscripts on the control and output coefficient matrices $\{B\}$ and $\{C\}$ refer to those coefficients associated with the controlled and residual mode, respectively. For a complete discussion of the assembly of this linear system matrix, the reader is referred to Ref 4.

For investigating system time response, eq 4 can be integrated. However, a root locus may be constructed from the open loop transfer function which has the form:

$$\frac{Y}{U} = \{C_c\}^T \left[s[I] - [A] \right]^{-1} \{B_c\} \qquad (5)$$

The matrices appearing in this formula may be obtained from the construction of the linear system model. The solution of eq 5 and the generation of the associated root locus diagram may be accomplished merely by loading the appropriate matrices into the "Total" program and executing the required options. An example of the use of "Total" for generation of the open loop transfer function and root locus diagram may be found in Appendix A.

To investigate a certain state weighting configuration or sensor type, the following steps were taken to produce a root locus diagram for analysis of control effectiveness. First, beam length, width, thickness, stiffness, and mass per unit length were selected. Sensor and actuator locations, type of sensor, observer pole offset, and state and control

-6-

weightings were input to the linear system model with the beam parameters. The *coefficient matrix in eq 4 was produced along* with the component matrices $[A_c]$, $[A_r]$, $\{B_c\}$, $\{B_r\}$, $\{C_c\}$, $\{C_r\}$, $\{G\}$, and $\{K\}$. At this point, if time response information was desired, the linear system model was numerically integrated. The matrices required for solution to eq 5 were loaded into "Total" and a root locus diagram was generated. For the investigation of classical control application, the same steps were followed. However, options of the "Total" program allow replacement of the feedback transfer function produced by the steady state optimal regulator with any desired transfer function.

EFFECT OF CHANGING ELEMENTS OF STATE WEIGHTING MATRIX

There have been several suggestions from various sources for picking the elements of the diagonal state weighting matrix [F] in the performance index:

$$J = 1/2 \int_0^\infty \left(\underline{v}_c^T [F] \underline{v}_c + f^T R f \right) dt \qquad (6)$$

For instance, Bryson and Ho (Ref. 2) present a scheme for selection of these elements based on the estimated maximum values of the states. Balas suggests energy weighting. Neither of these, when applied to the system in preliminary studies, yielded satisfactory response. The first investigation in this thesis, then, was a systematic exploration of the effect of changing each element of the state weighting matrix.

As a starting point, a configuration was selected that was previously shown to be stable using the weightings as picked by Hungerford. An aluminum beam 3 meters long, 3 cm wide and .5 cm thick was chosen. The observer poles were set ten units to the left of the average real value of the system poles. For the purpose of this examination, sensor and actuator locations were picked sufficiently far from any node to delete the effects of locating close to a node. On a 3 meter cantilever beam, a position sensor at 1.4 m from the clamped end and a force actuator at 0.6 m from the clamped end provides the desired conditions.

To begin the study, elements of the state weighting matrix were set to unity; that is

$$[F] \quad = \quad \text{Diag}[1 \quad 1 \quad 1 \quad 1] \tag{7}$$

The elements were separately varied from a value of .01 to 100, incremented by a factor of 10. Analysis of the results of variation about a base value of 1 suggested that a more suitable base value would be of order 10^2. Root locus diagrams for state weighting element variation from 1, Figs B1 to B5 in Appendix B, show significant changes only when elements are changed to 100. Unless otherwise noted, the root locus diagrams and time response results for this and all parts of the investigation are for unity gain. The gain is the coefficient k in the following equation:

$$u' \quad = \quad k \left\{ G \right\} \hat{\underline{v}}_c \tag{8}$$

where, again, u' is the control input, $\left\{ G \right\}$ is the feedback gain matrix, and $\hat{\underline{v}}_c$ is the controlled portion of the state vector.

To provide a more effective basis for the examination of effect of weighting charges, a new value was arbitrarily selected as a base from which each diagonal element was alternately varied. Since significant changes in the root locus were previously obtained with weightings of order 10^2, a value of 500 was selected as a new base value. Each diagonal element was set to 500, and in alternate executions of the computer program, each element was incremented from 500 to 1,000 to 2,000. Again, a root locus for each case may be found in Appendix B, Figs B6 to B9.

For these weighting variations, significant effects of

-9-

weighting changes were noticed in the root locus diagrams. The resulting movement of open loop zeroes in some case produced changes in the branch patterns. More importantly the closed loop pole locations for a unity gain system shifted significantly with respect to one another. For variations of the first two state weightings, these shifts were only slightly noticeable. Augmenting these first two state weighting elements to values of 10,000 and 100,000 produced more notable changes in the root locus diagrams.

At this point in the study it was realized that the value of the investigation was limited by a major problem with the investigative technique. Up to this point the third residual mode and the Luenberger observer were omitted when the component matrices were input to "Total" program. Although "Total" is capable of handling the 10 x 10 system resulting from four controlled mode states, four observer error states, and two residual mode states, the open loop transfer function produced had a 17th order polynomial numerator and an 18th order polynomial denominator. The order of this transfer function was too large to be processed by the "Total" program, so the residual mode and observer had been omitted. However, eight pole-zero cancellations occur because the forward loop transfer function zeroes are cancelled with the feedback transfer function poles. Omitting these poles and zeroes produced a transfer function small enough for the root locus generation by "Total". In this way the investigation was continued including the residual mode and the observer.

Figure 1 shows the resulting analysis performed on the

3 meter beam with the first two vibration modes controlled
and the third mode with no control applied. Each element of
the diagonal weighting matrix had a value of 500. The open
loop poles appear on the root locus as x's. The four open
loop poles grouped together near the real axis represent the
observer open loop poles. The three open loop poles located
on the imaginary axis represent the beam model with no nat-
ural damping, and their placement on the imaginary axis
represents the free vibration frequencies of each mode. The
small circles on the diagram represent open loop zeroes, and
the closed loop system poles for a gain of unity appear as
triangles. It is the relative positions of these closed loop
poles that is of interest in this investigation. Changes in
the locations of the closed loop poles on the branches extend-
ing from the imaginary axis represent changes in damping of
the associated mode. These changes are of particular interest
to this investigation.

The system that appears in Fig 1 serves as a basis for
comparison. State weighting matrix changes will produce
changes in closed loop pole locations from those in this fig-
ure. These shifts represent changes in the system response.
Changes in response can be verified by examination of time
response plots, which were obtained by numerical integration
of the system as formulated in Hungerford's program. Time
response plots of actuator force, displacement at sensor
location modal amplitudes of the first three modes, and the
percentage of the initial energy left in the beam can be
found in Appendix B, Figs B11 to B25, for each system

ROOT LOCUS FOR 3M BEAM
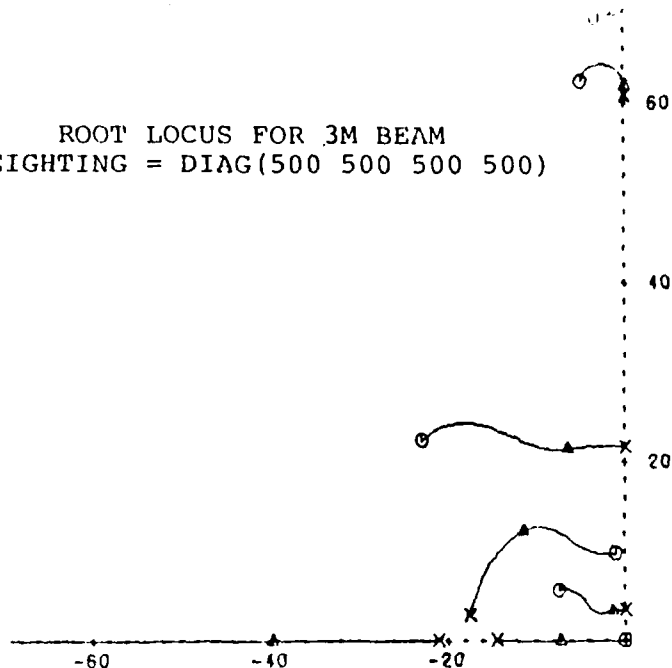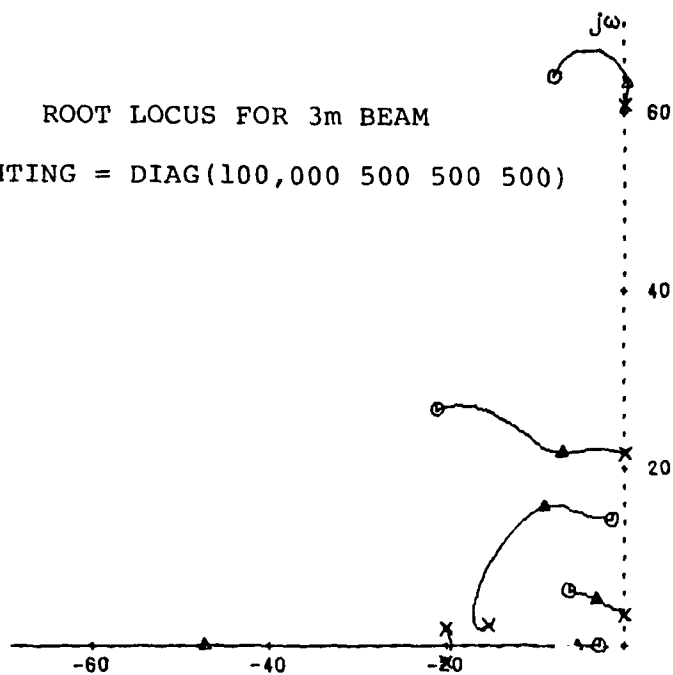WEIGHTING = DIAG(500 500 500 500)

Figure 1: Root locus diagram for base weighting configuration.

discussed in this section.

As before, weightings in the diagonal state weighting
matrix were changed alternately, with one element varied as
the other three stayed fixed at a value of 500. The amount
of augmentation of each element was based on the previous
analysis omitting the observer and residual mode.

A root locus for a diagonal weighting matrix with the
first state weighting of 100,000 and the remaining weights at
500 is shown in Fig 2a. The most obvious effect of this
heavy weighting on the first mode position state is the
shift to the left of the closed loop pole on the branch
starting at the first mode open loop pole. The effect of
such shift on system response is higher damping on first
mode vibrations, and examination of the time response plots,
Fig B15, verifies increased first mode damping. This weight-
ing also causes changes in the pattern of observer open loop

ROOT LOCUS FOR 3m BEAM

WEIGHTING = DIAG(100,000 500 500 500)
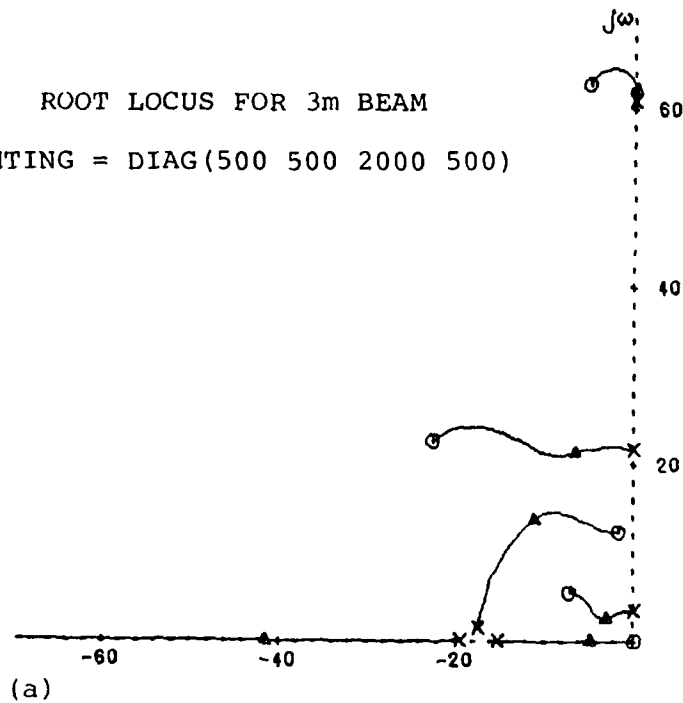
(a)

ROOT LOCUS FOR 3m BEAM

WEIGHTING = DIAG(500 10,000 500 500)
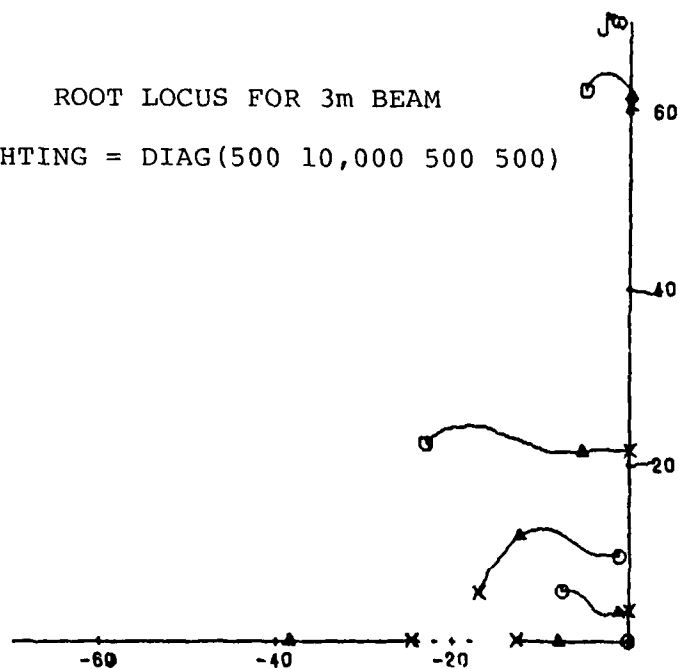
(b)

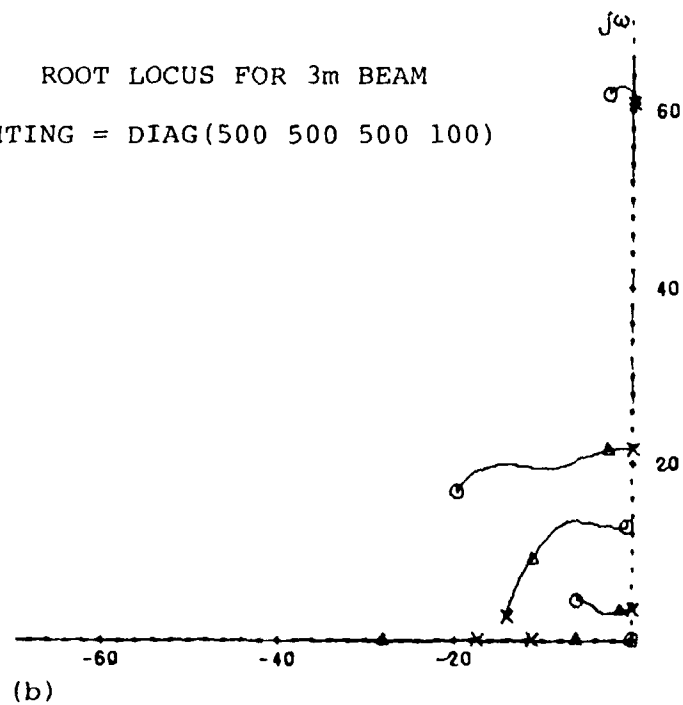Figure 2: Root locus diagrams for first two state weighting variations.

-13-

Figure 3: Root locus diagrams for second two state weighting variations.

-14-

pole positions; all four observer open loop poles are located off the real axis. This shift of observer poles causes a change in the branch patterns. The branch from the third mode open loop pole is moved closer to the imaginary axis, resulting in a shift to the right of the third mode closed loop pole and reduced damping the third mode. Examination of the time response plots, Fig B16, shows reduced damping in the third mode for heavy weighting of the first state.

Second state weighting was augmented to a value of 10,000, as shown in Fig 2b. In this case, augmentation of the weighting produced no noticeable changes in the closed loop pole locations, and no noticeable changes in the time response. The observer open loop poles, however, have been shifted farther away from each other. Augmenting this weighting to a value of 100,000 produces further separation of these observer poles, which causes a shift in the third mode branch into the right half plane and instability results.

As with increased first state weighting, increasing the third state weighting produces a shift to the left of the first mode closed loop pole, as in Fig 3a. Time response plots for the first two modes are nearly identical for a first state weighting of 100,000 and the third state weighting of 2,000. This indicates that the same behavior can be produced with heavy weightings on position state or relatively light weighting on the corresponding velocity state. The behavior of the observer poles is not similar for the two cases; for the third state weighting increase, the observer open loop pole locations are not significantly shifted. Consequently, the third mode

branch of the root locus in Fig 3a has not been significantly
shifted from its position when all weightings have a value of
500. Third mode time response plots, Figs B20, B21 and B22
verify that response of this mode does not significantly
change when the third state weighting is increased to 2,000.

When the fourth state weighting is increased from a value
of 500, the observer open loop poles shift off the real axis.
As in previous cases, this causes a critical shift in the
third mode branch pattern, and for unity gain an unstable
system results. To investigate the effect of changing this
fourth state weighting, the value was decreased from the base
value of 500 rather than increased. Figure 3b shows a root
locus diagram for the fourth state weighting of 100. A shift
to the right of the second mode closed loop pole resulted,
indicating the expected decreased damping of the second vi-
bration mode. The time response plots of this second mode,
Fig B24, shows decreased damping. The shift of this closed
loop pole had sufficient numerical impact to cause a decrease
in the average of the real part of the closed loop system
poles for unity gain. Since the observer open loop poles are
picked to be ten units to the left of the average real part,
the open loop observer poles are shifted to the right. The
resulting shift in the branch patterns produced higher damp-
ing of the third mode for unity gain, as exhibited in the
third mode time response plot, Fig B25.

The results of this part of the study can be summarized
by examining the effects of weighting changes on the closed
loop vibration mode poles and the open loop observer poles.

-16-

When an element of the state weighting matrix is increased with respect to the other elements, the associated closed loop pole reflects this increase in a shift to the left, indicating increased damping. For instance, relative increases in the first and third state weightings move the first mode closed loop pole to the left. Larger relative increases of the position state weightings are required to produce the same closed loop pole shift as a smaller relative velocity state weighting increase. There is a numerical limit to the tolerable amount of relative increase peculiar to each state weighting element and the relative magnitudes of the weighting configuration. When this limit is approached the mechanism for choosing open loop observer poles produces an increasingly scattered pattern of pole placement. This scattered pattern may cause an outward shift of higher mode closed loop poles, and instability may result for increasingly scattered patterns.

CLASSICAL FEEDBACK COMPENSATION APPLIED TO VIBRATING BEAM

The steady state optimal regulator provides a method for controlling bending vibration in a beam optimally through minimization of a performance index. As evidenced in the previous section, the choice of weightings in this performance index predetermines the limits of optimization; in some cases, the optimum was still an unstable system. Although intelligent selection of weightings can produce effective control, an alternative control law may also effectively control bending vibrations in a cantilever beam.

In applying the "Total" root locus generator during investigation of state weighting changes, it became apparent that selection of location of open loop poles and zeroes was the net effect of the application of the optimal regulator control law. The purpose of the investigation of classical control was to determine if satisfactory control of cantilever beam bending vibrations might be obtained by using classical feedback techniques as an alternative to the modern optimal control theory.

Classical feedback compensation as applied to bending vibrations in a cantilever beam deals with the relationships of the locations of system open loop poles and zeroes. By adding poles or zeroes at specified positions on a system root locus, branch patterns can be moved. The root locus of the system for a 3 m beam as described in the previous section and a steady state optimal regulator with all state weightings set to 500 is shown in Fig 4a. Sensor and actuator positions

-18-

remain at 1.4 m and 0.6 m from the clamped end, respectively. The Luenberger observer has been omitted since the states need not be known in order to apply classical feedback compensation. Classical feedback compensation was applied by first removing the steady state optimal regulator poles and zeroes from the transfer function of the system in Fig 4a. A feedback compensation transfer function was constructed to add zeroes in the desired locations on the root locus. This feedback transfer function replaced the steady state optimal regulator in the linear system model.

The technique used in this investigation involved the use of state space input, transfer function manipulation, and root locus and time response options of the "Total" program. First, the system model for the open loop beam was produced by the execution of the digital computer linear system model developed by Hungerford. By using the state-space input options of "Total", the [A], {B}, and {C} matrices were loaded for the uncontrolled beam. These matrices constitute a 6 x 6 system of one position state and one velocity state for each of three modes. The forward-loop transfer function was generated from this information, and the desired feedback-loop transfer function was loaded using the transfer function manipulation options. The open-loop transfer function was generated and used to construct a root locus. Time response to step input plots generated by time response options may be found in Appendix B, Figs B26, B27, B28, and B29. A comparison criterion was applied to these time response plots. Time

ROOT LOCUS FOR 3m BEAM

WEIGHTING = DIAG(500 500 500 500)

NO OBSERVER

(a)
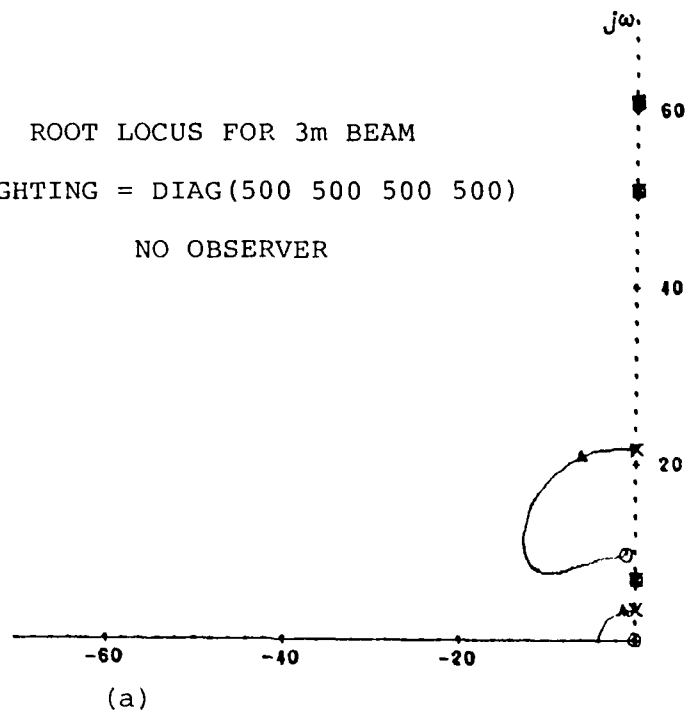
ROOT LOCUS FOR 3m BEAM

FEEDBACK COMPENSATION = S

GAIN = 35

(b)
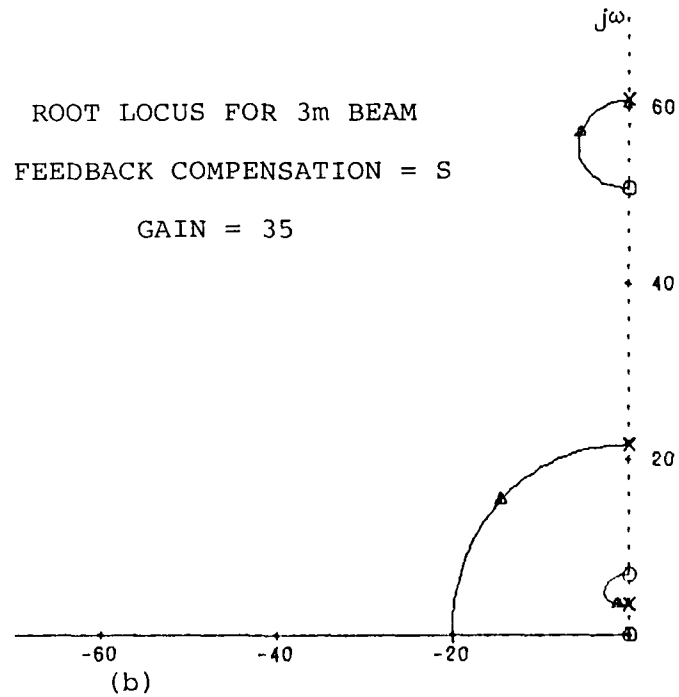
Figure 4:   Root locus diagrams for base weighting and feeback compensation.

ROOT LOCUS FOR 3m BEAM

FEEDBACK COMPENSATION = S + 50

GAIN = 1

(a)

ROOT LOCUS FOR 3m BEAM

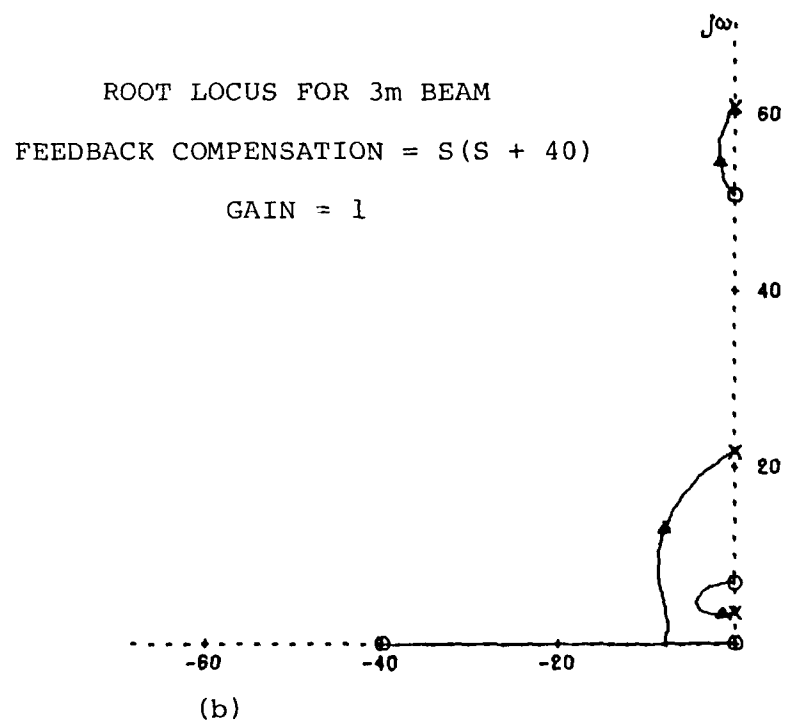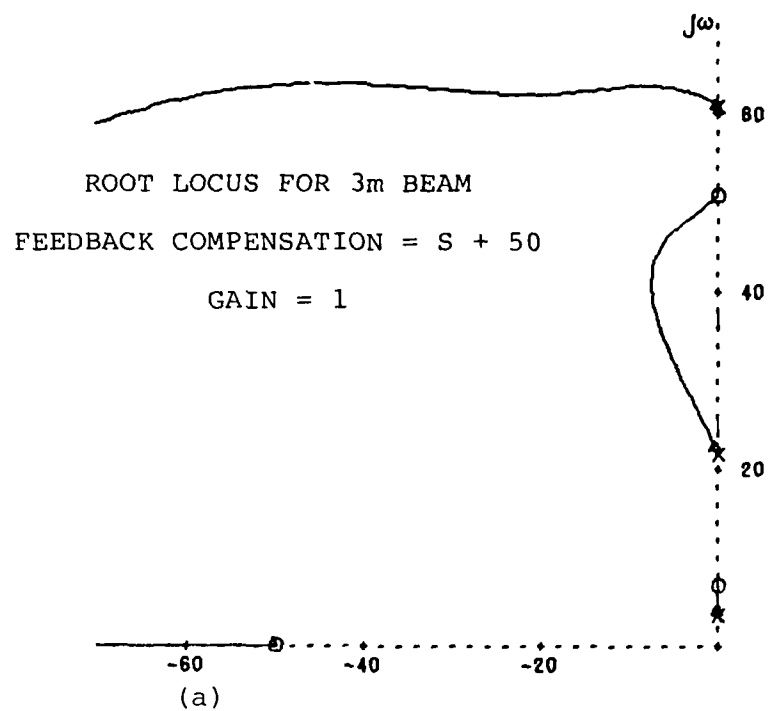FEEDBACK COMPENSATION = S(S + 40)

GAIN = 1

(b)

Figure 5: Root locus diagrams for feedback compensation.

to settle to within 5% of the final sensor displacement for a step input was selected as the comparison criterion for this investigation.

After examining Fig 4a, it was decided that favorable response characteristics might be obtained by pulling the branches toward the left of the root locus after removing the optimal regulator poles and zeroes. Classical feedback compensation rules suggest that root locus branches may be moved to the left by the addition of zeroes to the system (Ref 3). The simplest application of the rule is the addition of one zero. On a root locus diagram, the transfer function s + a places a zero on the real axis at -a. Root locus diagrams were produced and studied for location of this zero at the origin and 2, 4, 6, 8, 10, 20, 30, 40, and 50 units to the left of the origin on the real axis. Figure 4b shows the root locus for a = 0, and Fig 5a is a root locus for a = 50. As expected, the branch patterns in both cases are moved to the left. However, small values of "a" move the lower frequency branches more, and higher values of "a" have a greater effect on the higher frequencies. Figure 4b represents the former case, and Fig 5b represents the latter. Thus, when "a" is zero and the gain is 35, the time to settle to within 5% of final displacement is 3.2 sec, as shown in Fig B26. The same settling time is 3.0 sec when the steady state optimal regulator is applied with all state weightings equal to 500, as shown in Fig B27. When "a" is 50, there is little first mode damping and the 5% settling time is nearly infinite, as shown in Fig B28.

It was found that a zero near the origin affected low

-22-

frequencies and a zero far to the left of the origin affected
high frequencies. An attempt was made to affect both by add-
ing two zeroes. One zero was placed at the origin and a second
zero was added to produce the transfer function $s(s + a)$.
Root locus diagrams were studied for location of the second
zero at 20, 40, 60, and 80. Figure 5b shows the unity gain
closed loop poles when $a = 40$, which is representative of the
considered cases. The 5% settling time for this compensation
is 2.2 sec, as shown in Fig B29.

RATE AND POSITION-RATE SENSORS

For a cantilever beam in bending vibration with the first
three modes considered and the first two modes controlled and
observed, the resulting linear system model, as before, has
ten states. There are two controlled mode position states,
two controlled mode velocity states, four observer error
states, and one residual mode position state and velocity
state. The output matrix $\{C\}$ determines the nature of the
output y; for Hungerford's study and the previous portions
of this study the $\{C\}$ matrix for a position sensor had the
following form:

$$\{c_1 \ c_2 \ 0 \ 0 \ \vdots \ 0 \ 0 \ 0 \ 0 \ \vdots \ c_5 \ 0\} \tag{12}$$

The more general form of $\{C\}$ is

$$\{c_1 \ c_2 \ c_3 \ c_4 \ \vdots \ 0 \ 0 \ 0 \ 0 \ \vdots \ c_5 \ c_6\} \tag{13}$$

For a rate sensor, c_1, c_2, and c_5 are zero, and for a sensor
providing a combination of position and rate information, c_1
through c_6 are non-zero. An attempt was made to examine the
use of a rate sensor and a position-rate sensor in the linear
system model of the vibrating beam.

Changing from a position sensor required a substantial
modification of the linear system model as compiled by Hungerford.
The observer gain matrix $\{K\}$ was found by setting the eigenvalues
of the matrix $[A-\{K\}\{C\}]$ equal to a desired set of eigenvalues.
The resulting linear equation is simplified when c_3, c_4 and
c_6 are zero. The more general case requires the solution of
more complicated system of linear equations:

-24-

$$\begin{bmatrix} c_1 & c_2 & c_3 & c_4 \\ -\omega_1^2 c_3 & -\omega_2^2 c_4 & c_1 & c_2 \\ c_1 \omega_2^2 & c_2 \omega_1^2 & c_3 \omega_2^2 & c_4 \omega_1^2 \\ -c_3 \omega_1^2 \omega_2^2 & -c_4 \omega_1^2 \omega_2^2 & c_1 \omega_2^2 & c_2 \omega_1^2 \end{bmatrix} \begin{bmatrix} K_1 \\ K_2 \\ K_3 \\ K_4 \end{bmatrix} = \begin{bmatrix} H_3 \\ H_2 - \omega_1^2 - \omega_2^2 \\ H_1 \\ H_0 - \omega_1^2 \omega_2^2 \end{bmatrix} \quad (14)$$

$$H_3 = r_1 + r_2 + r_3 + r_4$$

$$H_2 = r_1(r_2 + r_3 + r_4) + r_2(r_3 + r_4) + r_3 r_4$$

$$H_1 = r_4(r_1 r_2 + r_1 r_3 + r_2 r_3) + r_1 r_2 r_3$$

$$H_0 = r_1 r_2 r_3 r_4$$

In equations (14), r_1, r_2, r_3, and r_4 are the desired observer eigenvalues. Solution of (14) using a library linear equation solving routine allowed a choice of sensor type.

For this part of the study, a beam one meter long was used. All other parameters were kept the same as those in the first part of this investigation, with all state weightings equal to 500. Sensor and actuator positions were varied along the length of the beam at 0.2 m intervals, and the linear system model compiled for each configuration. This was done for a position sensor, a rate sensor, and a position-rate sensor. The eigenvalues of corresponding systems were compared for stability information. Computer model outputs for three different sensors at 0.6 m and actuator at 0.4 m given in Appendix C.

It was found that including rate information in the sensor
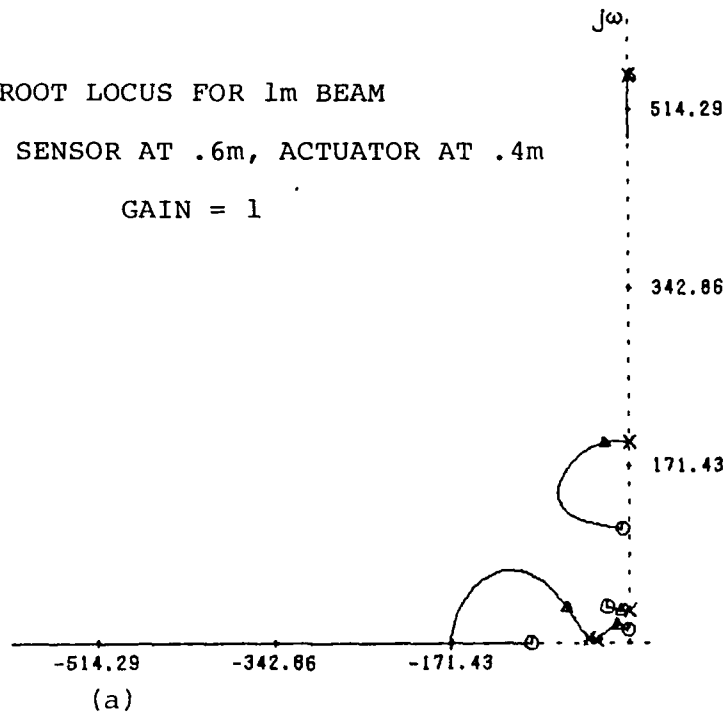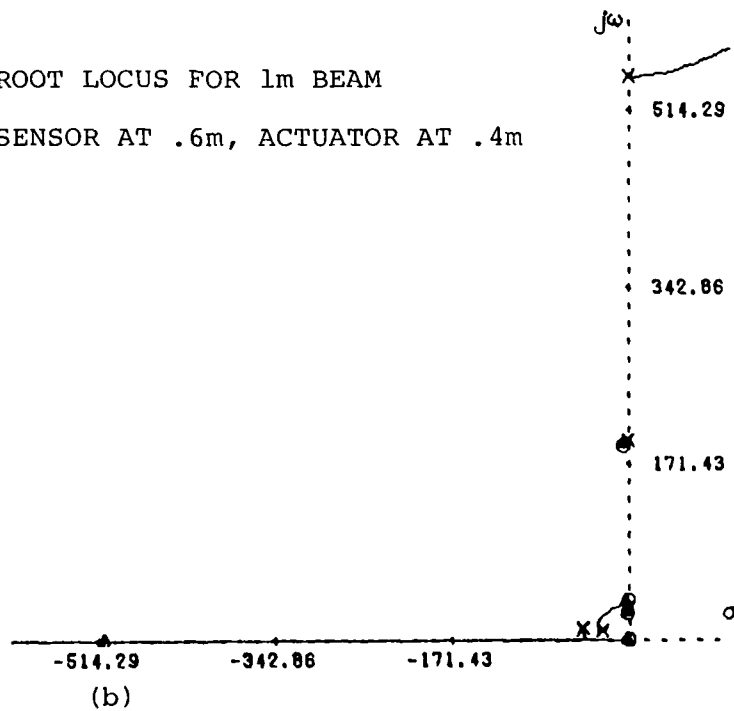
Figure 6: Root locus diagrams for position and rate sensors.

model caused unstable third mode vibrations. This instability results directly from stiffness and ill-conditioning of the linear system of equations that is solved for observer gains. A comparison of root locus diagrams for a beam with sensor at 0.6 m and actuator at 0.4 m with position and rate sensors appears in Fig 6. Although the closed loop observer eigenvalues are the same for both systems, the figure shows a shift in open loop observer poles that causes a shift to the right of the open loop zeroes when rate information is sensed.

CONCLUSION

1. Damping of a controlled mode can be changed by making a change in the corresponding position or velocity state weighting matrix element in the quadratic performance index of the steady state optimal regulator. The rest of the system remains unaffected unless the value of this element approaches the numerical limits of the model. At this limit, the observer model begins to break down.

2. Classical feedback compensation applied through addition of open loop zeroes to the system root locus can provide effective control of bending vibrations in a cantilever beam.

3. The observer model is adversely affected when rate information is included in the sensor model, whether this model includes rate and position sensing or rate sensing alone.

RECOMMENDATIONS

1. The study of state weighting element changes was limited to a beam with two controlled modes and one residual mode by limitations of the "Total" program. The study should be expanded to consider a higher number of modes, perhaps by expanding the capability of this package.

2. Based on the relationships discovered in this investigation and in Hungerford's work, control effectiveness of combinations of state and control weighting, observer pole offsett, and sensor and actuator locations should be investigated.

3. Classical feedback compensation should be applied to very long beams. Hungerford found that the optimal regulator had difficulty with long beams. The results of this investigation suggest that classical control may be more effective because of increased numerical simplicity.

4. Classical feedback compensation should be applied to a beam model that includes a higher number of modes and higher frequency vibrations. The use of more complex types of compensation may also warrant investigation. Other sensor and actuator locations than the ones used in this study should be investigated using classical compensation.

BIBLIOGRAPHY

1. Balas, M.J., "Active Control of Flexible Systems "AIAA Symposium on Dynamics and Control of Large Flexible Spacecraft, Blacksburg, June 14, 1977.

2. Bryson, Arthur E., and Yu-Chi Ho, Applied Optimal Control, Waltham, Mass.: Blaisdell Publishing Company, 1969.

3. D'Azzo, John J., and Constantine H. Houpis, Linear Control System Analysis and Design, New York: McGraw-Hill Book Company, 1975.

4. Hungerford, John B., "Active Control of Bending Vibration in a Cantilever Beam", Air Force Institute of Technology thesis AFIT/GA/AA/77D-7, 1977.

5. Larimer, Stanley J., "User's Manual for Total", AFIT digital computer package user's guide, 1978.

APPENDICES

Appendix A

Typical Use of the AFIT "Total" Package

The following pages are a listing of a typical session with the interaction computer-aided design program for control system analysis called "Total". Options in the package are selected by a numerical input, and the lists of options used can be found at convenient locations in the listing.

```
ATTACH,TOTAL,ID=AFIT

 PFN IS
 TOTAL
 PF CYCLE NO. = 001
COMMAND- TOTAL

WELCOME TO TOTAL--VERSION 1.4
TYPE HELP FOR INTRO, TYPE 99 FOR NEW FEATURES BULLETIN

OPTION >  10


(10-19) MATRIX INPUT OPTIONS
* 10     LIST OPTIONS
* 11     AMAT   CONTINUOUS SYSTEM MATRIX
* 12     BMAT   CONTINUOUS INPUT DISTRIBUTION MATRIX
* 13     CMAT   OUTPUT CONTRIBUTION MATRIX
* 14     DMAT   DIRECT TRANSMISSION MATRIX
* 15     KMAT   ST. VAR. FEEDBACK MATRIX
* 16     FMAT   DISCRETE SYSTEM MATRIX
* 17     GMAT   DISCRETE INPUT DISTRIBUTION MATRIX
* 18     HELP USER SET UP STATE-SPACE MODEL OF SYSTEM
* 19     EXPLAIN USE OF ABOVE MATRICIES

OPTION >  18

IS THE SYSTEM (1) CONTINUOUS OR (2) DISCRETE? >    1


THE EQUATIONS YOU ARE ABOUT TO INPUT HAVE THE FORM:

                XDOT(T) = [ AMAT ]X(T) + [ BMAT ]U(T)
                   Y(T) = [ CMAT ]X(T) + [ DMAT ]U(T)
    WHERE          U(T) =  GAIN*( R(T) - [ KMAT ]X(T) )

AND    X   IS A VECTOR OF  N   STATE VARIABLES
       U   IS A VECTOR OF  M   INPUTS
       Y   IS A VECTOR OF  L   OUTPUTS

ENTER NO. OF STATES,INPUTS,OUTPUTS >  10,1,1

ENTER AMAT WITH 10 ROWS AND 10 COLUMNS.

ENTER 10 ELEMENTS PER ROW:
ROW 1 > 0 0 1 0 0 0 0 0 0 0

ROW 2 > 0 0 0 1 0 0 0 0 0 0

ROW 3 > -12.002 0 0 0 0 0 0 0 0 0

ROW 4 > 0 -471.433 0 0 0 0 0 0 0 0

ROW 5 > 0 0 0 0 -44.73 106.9 1 0 30.16 0

ROW 6 > 0 0 0 0 10.6 -25.31 0 1 -7.14 0

ROW 7 > 0 0 0 0 -167.3 371.0 0 0 104.7 0

ROW 8 > 0 0 0 0 501.7 -1670 0 0 -338.3 0

ROW 9 > 0 0 0 0 0 0 0 0 0 1
```

COL >	1	2	3	4	5
ROW					
1	0.	0.	1.000	0.	0.
2	0.	0.	0.	1.000	0.
3	-12.00	0.	0.	0.	0.
4	0.	-471.4	0.	0.	0.
5	0.	0.	0.	0.	-44.73
6	0.	0.	0.	0.	10.60
7	0.	0.	0.	0.	-167.3
8	0.	0.	0.	0.	501.7
9	0.	0.	0.	0.	0.
10	0.	0.	0.	0.	0.

COL >	6	7	8	9	10
ROW					
1	0.	0.	0.	0.	0.
2	0.	0.	0.	0.	0.
3	0.	0.	0.	0.	0.
4	0.	0.	0.	0.	0.
5	106.9	1.000	0.	30.16	0.
6	-25.31	0.	1.000	-7.140	0.
7	371.0	0.	0.	104.7	0.
8	-1670.	0.	0.	-338.3	0.
9	0.	0.	0.	0.	1.000
10	0.	0.	0.	-3697.	0.

ENTER BMAT WITH 10 ROWS AND 1 COLUMNS.

ENTER 10 ELEMENTS PER COLUMN:
COLUMN 1 > 0 0 -.1174 .5535 0 0 0 0 0 -1.112

COL >	1
ROW	
1	0.
2	0.
3	-.1174
4	.5535
5	0.
6	0.
7	0.
8	0.
9	0.
10	-1.112

ENTER CMAT WITH 1 ROWS AND 10 COLUMNS.

ENTER 10 ELEMENTS PER ROW:
ROW 1 > -.5542 1.324 0 0 0 0 0 0 -.3737 0

COL >	1	2	3	4	5
ROW					
1	-.5542	1.324	0.	0.	0.

```
     COL >     6             7             8              9            10
ROW
  1        0.            0.            0.            -.3737         0.
```

IS THERE A DIRECT-TRANSMISSION (D MATRIX)--YES OR NO? >   NO

DMAT SET TO 1 BY 1 ZERO MATRIX (OPTION 78)
IS THERE A STATE-VARIABLE FEEDBACK MATRIX--YES OR NO? >   YES

ENTER KMAT WITH 1 ROWS AND 10 COLUMNS.

ENTER 10 ELEMENTS PER ROW:
ROW 1 > 10.88 111.1 -45.1 21.8 10.88 111.1 -45.1 21.8 0 0

```
     COL >     1             2             3              4            5
ROW
  1        10.88         111.1         -45.10         21.80        10.88
```

```
     COL >     6             7             8              9            10
ROW
  1        111.1         -45.10        221.80         0.           0.
```

THE STATE-SPACE REPRESENTATION IS COMPLETE.

OPTION >   20

(20-29) BLOCK DIAGRAM MANIPULATION OPTIONS
* 20   LIST OPTIONS
* 21   FORM OLTF = GTF * HTF   (IN CASCADE)
* 22   FORM CLTF = (GAIN*GTF)/(1 + GAIN*GTF*HTF)
* 23   FORM CLTF = GAIN*OLTF / (1 + GAIN*OLTF)
* 24   FORM CLTF = GTF + HTF   (IN PARALLEL)
* 25   GTF(S) & HTF(S) FROM CONTINUOUS STATE-SPACE MODEL
* 26   GTF(Z) & HTF(Z) FROM DISCRETE STATE-SPACE MODEL
* 27   WRITE ADJOINT(SI-AMAT) TO FILE ANSWER
* 28   FIND HTF FROM CLTF & GTF (FOR CLTF=GTF*HTF/(1+GTF*HTF))
* 29   FIND HTF FROM CLTF & GTF (FOR CLTF= GTF /(1+GTF*HTF))

OPTION >   25

GTF(S) AND HTF(S) CALCULATED FROM STATE-SPACE
TYPE: GTF   OR   HTF   FOR RESULTS

FORWARD-LOOP TRANSFER FUNCTION

$$GK = (\ GNK/GDK\ ) = \quad 1.213$$

GTF(S) NUMERATOR

I	GNPOLY(I)		GZERO(I)			
1	(1.213	)S** 8	(.8688E-11)	+	J(6.880	)
2	(84.99	)S** 7	(.8670E-11)	+	J(-6.880	)
3	(5418.	)S** 6	(-19.81)	+	J(1.554	)
4	(.2494E+06)	S** 5	(-19.81)	+	J(-1.554	)
5	(.6119E+07)	S** 4	(-15.21)	+	J(2.205	)
6	(.7856E+08)	S** 3	(-15.21)	+	J(-2.205	)
7	(.5698E+09)	S** 2	(-.4079E-12)	+	J(50.81	)
8	(.3168E+10)	S** 1	(-.4079E-12)	+	J(-50.81	)
9	(.1383E+11)		GNK=		1.213	

GTF(S) DENOMINATOR

I	GDPOLY(I)		GPOLE(I)			
1	(1.000	)S**10	(-.1916E-09)	+	J(3.464	)
2	(70.04	)S** 9	(-.1916E-09)	+	J(-3.464	)
3	(6017.	)S** 8	(-19.81)	+	J(-1.554	)
4	(.3142E+06)	S** 7	(-19.81)	+	J(1.554	)
5	(.9563E+07)	S** 6	(-15.21)	+	J(-2.205	)
6	(.2149E+09)	S** 5	(-15.21)	+	J(2.205	)
7	(.3703E+10)	S** 4	(.1402E-11)	+	J(-21.71	)
8	(.3978E+11)	S** 3	(.1398E-11)	+	J(21.71	)
9	(.2056E+12)	S** 2	(-.2216E-12)	+	J(60.80	)
10	(.4470E+12)	S** 1	(-.2216E-12)	+	J(-60.80	)
11	(.1951E+13)		GDK=		1.000	

OPTION > HTF

FEEDBACK-LOOP TRANSFER FUNCTION

$$HK = (\ HNK/HDK\ ) = \quad 14.31$$

HTF(S) NUMERATOR

I	HNPOLY(I)		HZERO(I)			
1	(17.36	)S** 9	(.8111E-02)	+	J(0.	)
2	(1276.	)S** 8	(-7.386)	+	J(5.583	)
3	(.1169E+06)	S** 7	(-7.386)	+	J(-5.583	)
4	(.5326E+07)	S** 6	(-1.689)	+	J(-12.35	)
5	(.1601E+09)	S** 5	(-1.689)	+	J(12.35	)
6	(.2489E+10)	S** 4	(-22.63)	+	J(-22.62	)
7	(.3020E+11)	S** 3	(-22.63)	+	J(22.62	)
8	(.2253E+12)	S** 2	(-5.053)	+	J(-62.70	)
9	(.9350E+12)	S** 1	(-5.053)	+	J(62.70	)
10	(-.7598E+10)		HNK=		17.36	

HTF(S) DENOMINATOR

I	HDPOLY(I)		HPOLE(I)			
1	(1.213	)S** 8	(.8688E-11)	+	J(6.880	)
2	(84.99	)S** 7	(.8670E-11)	+	J(-6.880	)
3	(5418.	)S** 6	(-19.81)	+	J(1.554	)
4	(.2494E+06)	S** 5	(-19.81)	+	J(-1.554	)
5	(.6119E+07)	S** 4	(-15.21)	+	J(2.205	)
6	(.7856E+08)	S** 3	(-15.21)	+	J(-2.205	)
7	(.5698E+09)	S** 2	(-.4079E-12)	+	J(50.81	)
8	(.3168E+10)	S** 1	(-.4079E-12)	+	J(-50.81	)

OPTION > 21

OPTION >
OLTF.

OPEN-LOOP TRANSFER FUNCTION

$$OLK= GAIN*(OLNK/OLDK)= \quad 17.36$$
$$GAIN= \quad 1.000$$

OLTF(S) NUMERATOR

I	OLNPOLY(I)		OLZERO(I)			
1	(	21.07)S**17	(	.8111E-02) + J(	0.	)
2	(	3024.)S**16	(	-7.386) + J(	5.583	)
3	(	.3444E+06)S**15	(	-7.386) + J(	-5.583	)
4	(	.2764E+08)S**14	(	.8840E-11) + J(	-6.880	)
5	(	.1705E+10)S**13	(	.8839E-11) + J(	6.880	)
6	(	.8381E+11)S**12	(	-15.21) + J(	2.205	)
7	(	.3269E+13)S**11	(	-15.21) + J(	-2.205	)
8	(	.9882E+14)S**10	(	-1.689) + J(	-12.35	)
9	(	.2274E+16)S** 9	(	-1.689) + J(	12.35	)
10	(	.4007E+17)S** 8	(	-19.81) + J(	-1.554	)
11	(	.5513E+18)S** 7	(	-19.81) + J(	1.554	)
12	(	.5984E+19)S** 6	(	-22.63) + J(	-22.62	)
13	(	.5073E+20)S** 5	(	-22.63) + J(	22.62	)
14	(	.3319E+21)S** 4	(	-.2142E-11) + J(	-50.81	)
15	(	.1664E+22)S** 3	(	-.2104E-11) + J(	50.81	)
16	(	.6074E+22)S** 2	(	-5.053) + J(	-62.70	)
17	(	.1290E+23)S** 1	(	-5.053) + J(	62.70	)
18	(	-.1051E+21)		OLNK=	21.07	

OLTF(S) DENOMINATOR

I	OLDPOLY(I)		OLPOLE(I)			
1	(	1.213)S**18	(	-.1916E-09) + J(	3.464	)
2	(	170.0)S**17	(	-.1916E-09) + J(	-3.464	)
3	(	.1867E+05)S**16	(	-15.21) + J(	-2.205	)
4	(	.1521E+07)S**15	(	-15.21) + J(	2.205	)
5	(	.9449E+08)S**14	(	.8546E-11) + J(	6.880	)
6	(	.4783E+10)S**13	(	.8546E-11) + J(	-6.880	)
7	(	.1958E+12)S**12	(	-19.81) + J(	1.554	)
8	(	.6350E+13)S**11	(	-19.81) + J(	-1.554	)
9	(	.1641E+15)S**10	(	-19.81) + J(	1.553	)
10	(	.3422E+16)S** 9	(	-19.81) + J(	-1.553	)
11	(	.5714E+17)S** 8	(	-15.21) + J(	2.206	)
12	(	.7453E+18)S** 7	(	-15.21) + J(	-2.206	)
13	(	.7428E+19)S** 6	(	.1654E-11) + J(	21.71	)
14	(	.5674E+20)S** 5	(	.1656E-11) + J(	-21.71	)
15	(	.3414E+21)S** 4	(	-.9013E-12) + J(	50.81	)
16	(	.1609E+22)S** 3	(	-.1101E-11) + J(	-50.81	)
17	(	.5371E+22)S** 2	(	.5889E-12) + J(	60.80	)
18	(	.1236E+23)S** 1	(	.5889E-12) + J(	-60.80	)
19	(	.2697E+23)		OLDK=	1.213	

FACTORED INPUT OF OLTF
ENTER NUM & DENOM DEGREES (OR SOURCE): 9,10

ENTER NUMERATOR CONSTANT: 21.07

ENTER EACH ROOT--RE,IM
OLZERO(1)= .0081111,0
OLZERO(2)= -7.386,5.583
OLZERO(3)= (-7.386   ) + J(-5.583   ) ASSUMED
OLZERO(4)= -1.688,12;35
OLZERO(5)= (-1.689   ) + J(-12.35   ) ASSUMED
OLZERO(6)= -22.63,22.62
OLZERO(7)= (-22.63   ) + J(-22.62   ) ASSUMED
OLZERO(8)= -5.053,62.7
OLZERO(9)= (-5.053   ) + J(-62.70   ) ASSUMED

OLTF NUMERATOR (OLNPOLY)   OLTF ZEROS (OLZERO)
(21.07   )S** 9   (.8111E-02) + J(0.   )
(1549.   )S** 8   (-7.386   ) + J(5.583   )
(.1419E+06)S** 7   (-7.386   ) + J(-5.583   )
(.6464E+07)S** 6   (-1.689   ) + J(12.35   )
(.1944E+09)S** 5   (-1.689   ) + J(-12.35   )
(.3021E+10)S** 4   (-22.63   ) + J(22.62   )
(.3666E+11)S** 3   (-22.63   ) + J(-22.62   )
(.2735E+12)S** 2   (-5.053   ) + J(62.70   )
(.1135E+13)S** 1   (-5.053   ) + J(-62.70   )
(-.9221E+10)   POLYNOMIAL CONSTANT=   21.07

ENTER DENOMINATOR CONSTANT: 1.213

ENTER EACH ROOT--RE,IM
OLPOLE(1)= 0,3.464
OLPOLE(2)= (0.   ) + J(-3.464   ) ASSUMED
OLPOLE(3)= -19.81,1.553
OLPOLE(4)= (-19.81   ) + J(-1.553   ) ASSUMED
OLPOLE(5)= -15.21,2.206
OLPOLE(6)= (-15.21   ) + J(-2.206   ) ASSUMED
OLPOLE(7)= 0,21.71
OLPOLE(8)= (0.   ) + J(-21.71   ) ASSUMED
OLPOLE(9)= 0,60.8
OLPOLE(10)= (0.   ) + J(-60.80   ) ASSUMED

OLTF DENOMINATOR (OLDPOLY)   OLTF POLES (OLPOLE)
(1.213   )S**10   (0.   ) + J(3.464   )
(84.96   )S** 9   (0.   ) + J(-3.464   )
(7298.   )S** 8   (-19.81   ) + J(1.553   )
(.3810E+06)S** 7   (-19.81   ) + J(-1.553   )
(.1160E+08)S** 6   (-15.21   ) + J(2.206   )
(.2606E+09)S** 5   (-15.21   ) + J(-2.206   )
(.4491E+10)S** 4   (0.   ) + J(21.71   )
(.4824E+11)S** 3   (0.   ) + J(-21.71   )
(.2493E+12)S** 2   (0.   ) + J(60.80   )
(.5419E+12)S** 1   (0.   ) + J(-60.80   )
(.2365E+13)   POLYNOMIAL CONSTANT=   1.213

GAIN= 1.0   OLK= GAIN*(OLNK/OLDK)= 17.37015663644

OPTION >   AA=10   THESE COMMANDS SET THE PLOT BOUNDARIES

AA=   10.00000000

OPTION >   BB=70

-38-

```
BB=        70.00000000

OPTION >   DD=-70

DD=       -70.00000000

OPTION >   PLOT,ON


OPTION >   ANSWER,ON

ANSWER ON--OUTPUT WILL GO TO FILE--ANSWER

OPTION >   42

ENTER GAIN OF INTEREST (GAIN),TOLERANCE (GTOL):>   1,.01


TITLE OF THIS PARTICULAR PLOT--PRINTED INSIDE BOX:
> [--------ENTER TITLE   (50 CHARACTERS MAX)--------] <
>   ROOT LOCUS, 3M BEAM   WT = DIAG(500 500 500 2000)

    ROOT LOCUS, 3M BEAM   WT = DIAG(500 500 500 2000)

OPTION >   STOP

LOCAL FILE--PLOT--CONTAINS CALCOMP PLOT(S)
LOCAL FILE--ANSWER--CONTAINS OUTPUT
ALL INFO IN TOTAL HAS BEEN SAVED IN LOCAL FILE--MEMORY.
     STOP
     9.632 CP SECONDS EXECUTION TIME
COMMAND- ROUTE,PLOT,ST=CSB,DC=PT,TID=BB

COMMAND- ROUTE,ANSWER,DC=PR,ST=CSB,TID=BB,FID=F11

COMMAND- LOGOUT
```

OPEN-LOOP (OLTF) ROOT LOCUS USING OPTION 42

    CODE
        0-LOCUS PT.   2-ZERO   4-IMAGINARY AXIS
        1-POLE   3-BREAK PT.   5-SENSITIVITY PT.

    10 POLES AT
        X =   0.   Y =   3.4840
        X =   0.   Y =   -3.4840
        X = -19.810   Y =   1.5530
        X = -19.810   Y =   -1.5530
        X = -15.210   Y =   2.2050
        X = -15.210   Y =   -2.2050
        X =   0.   Y =   21.710
        X =   0.   Y = -21.710
        X =   0.   Y =   60.800
        X =   0.   Y = -60.800

     3 ZEROS AT
        X =   .31111E-02   Y =   0.
        X =   -7.3850   Y =   5.5830
        X =   -7.3850   Y =   -5.5830
        X =   -1.6830   Y =   12.350
        X =   -1.6830   Y = -12.350
        X = -22.630   Y =   22.820
        X = -22.630   Y = -22.820
        X =   -5.0530   Y =   62.700
        X =   -5.0530   Y = -62.700

    GAIN CONSTANT (OLNK/OLDK)=   17.370157

    GAIN OF INTEREST (GAIN) =   1.000   +OR- GTOL =   .1000E-

    SENSITIVITY OF INTEREST (OLK) =   17.37   +OR- KTOL =   .1737

    ROOTS OF INTEREST
        X =   -3.1750   Y =   2.5015
        X =   -3.1350   Y =   -2.5015
        X =   -4.7211   Y =   0.
        X = -11.116   Y = -13.175
        X = -11.116   Y =   13.175
        X =   -5.4503   Y = -21.402
        X =   -5.4503   Y =   21.402
        X = -11.532   Y =   0.
        X =   .14375   Y = -62.245
        X =   .14375   Y =   62.245

    REGION OF CALCULATION-REAL: CC=   -90.0   TO AA=   10.0
                                 IMAJ: DD=   -70.0   TO BB=   70.0

                        BRANCH NUMBER   1

    CALCULATION STEP SIZE =   .5000

LOCUS REAL	LOCUS IMAG	DIST TO ORIGIN	GAIN	ZETA	CD
0.	3.4549300	3.4549030	0.	.00000	1
-3.0733427	2.5199754	4.7330874	.790251	.76213	
-3.2323154	2.5919452	4.1435637	1.01446	.78020	
-5.6051227	4.7502771	7.3355615	2.27050	.76570	
-7.3350000	5.5930000	9.2936654	0.	.79774	2

BRANCH NUMBER 2

```
CALCULATION STEP SIZE =  .8000
PRINTING STEP SIZE     = 4.000
```

LOCUS REAL	LOCUS IMAG	DIST TO ORIGIN	GAIN	ZETA	CD
0.	-3.4549300	3.4549003	0.	.00000	1
-3.0733427	-2.5199754	4.0330874	.990251	.76213	
-3.2323154	-2.5919452	4.1435637	1.01446	.78020	
-5.6051227	-4.7502771	7.3355615	2.27050	.76570	
-7.3350000	-5.5930000	9.2936654	0.	.79774	2

BRANCH NUMBER 3

```
CALCULATION STEP SIZE =  .8000
PRINTING STEP SIZE     = 4.000
```

LOCUS REAL	LOCUS IMAG	DIST TO ORIGIN	GAIN	ZETA	CD
-19.310000	1.5530000	19.370780	0.	.99694	1
-19.473547	0.	19.473547	.129935E-02	1.00000	2
-23.473547	0.	23.473547	.174462E-01	1.00000	0
-27.473547	0.	27.473547	.587254E-01	1.00000	0
-31.473547	0.	31.473547	.269939	1.00000	0
-35.473547	0.	35.473547	.521512	1.00000	0
-39.473547	0.	39.473547	.826712	1.00000	0
-41.373547	0.	41.573547	1.02433	1.00000	0
-45.233547	0.	45.233547	1.30914	1.00000	0
-49.233547	0.	49.233547	1.65059	1.00000	0
-53.233547	0.	53.233547	1.98770	1.00000	0
-57.233547	0.	57.233547	2.31665	1.00000	0
-61.233547	0.	61.233547	2.63649	1.00000	0
-65.233547	0.	65.233547	2.94727	1.00000	0
-69.233547	0.	69.233547	3.24939	1.00000	0
-73.233547	0.	73.233547	3.54459	1.00000	0
-77.233547	0.	77.233547	3.83281	1.00000	0
-81.233547	0.	81.233547	4.11517	1.00000	0
-85.233547	0.	85.233547	4.39240	1.00000	0
-89.233547	0.	89.233547	4.66511	1.00000	0
-90.033547	0.	90.033547	4.71916	1.00000	0

BOUNDARY

BRANCH NUMBER 4

```
CALCULATION STEP SIZE =  .8000
PRINTING STEP SIZE     = 4.000
```

LOCUS REAL	LOCUS IMAG	DIST TO ORIGIN	GAIN	ZETA	CD
-19.310000	-1.5530000	19.370780	0.	.99694	1
-19.473547	0.	19.473547	.129935E-02	1.00000	2
-15.473547	0.	15.473547	.764125E-02	1.00000	0
	0.	11.473547	.749354E-01	1.00000	0

PRANCH NUMBER   5

CALCULATION STEP SIZE = .8000
PRINTING STEP SIZE   = 4.000

LOCUS REAL	LOCUS IMAG	DIST TO ORIGIN	GAIN	ZETA	CO
-15.213000	2.2060000	15.359142	0.	.98855	1
-16.553709	4.5697023	17.277964	.166728E-01	.96439	0
-15.338631	8.3296576	17.454424	.160355	.87879	0
-13.120324	11.645207	17.544463	.594199	.74781	0
-10.772835	13.807080	17.512472	1.05778	.61515	5
-7.5580453	14.203564	16.094344	1.55155	.46953	0
-3.8554923	12.704745	13.276682	4.00795	.29040	0
-1.6333000	12.350000	12.464960	0.	.13550	2

PRANCH NUMBER   6

CALCULATION STEP SIZE = .8000
PRINTING STEP SIZE   = 4.000

LOCUS REAL	LOCUS IMAG	DIST TO ORIGIN	GAIN	ZETA	CO
-15.213000	-2.2060000	15.359142	0.	.98855	1
-16.553709	-4.5697023	17.277964	.166728E-01	.96439	0
-15.338631	-8.3296576	17.454424	.160955	.87879	0
-13.120324	-11.645207	17.544463	.594199	.74781	0
-10.772835	-13.807080	17.512472	1.05778	.61515	5
-7.5580453	-14.203564	16.094344	1.55155	.46953	0
-3.8554923	-12.704745	13.276682	4.00795	.29040	0
-1.6333000	-12.350000	12.464960	0.	.13550	2

PRANCH NUMBER   7

CALCULATION STEP SIZE = .8000
PRINTING STEP SIZE   = 4.000

LOCUS REAL	LOCUS IMAG	DIST TO ORIGIN	GAIN	ZETA	CO
0.	21.710000	21.710000	0.	.00000	1
-3.9739621	21.843017	22.207853	.543106	.17905	0
-7.1203757	21.291764	22.442904	1.08434	.31743	5
-10.170771	21.573767	22.952699	1.45150	.43523	0
-14.067117	23.275324	27.137205	2.22723	.51875	0
-17.003158	24.273725	30.150152	4.14249	.59750	0
-21.722571	23.710338	31.955651	17.5852	.63153	0
-22.530000	22.620000	31.936593	0.	.70725	2

PRANCH NUMBER   8

CALCULATION STEP SIZE = .8000
PRINTING STEP SIZE   = 4.000

LOCUS REAL	LOCUS IMAG	DIST TO ORIGIN	GAIN	ZETA	CO
0.	-21.710000	21.710000	0.	.00000	
-3.9739621	-21.843017	22.207853	.543106	.17905	

-17.400153	-24.477275	70.150157	6.16259	.59763	0
-21.232121	-27.719375	71.368451	17.5852	.63157	0
-22.650010	-22.020000	71.538533	0.	.70725	0

BRANCH NUMBER   9

CALCULATION STEP SIZE =   .8000
PRINTING STEP SIZE   = 4.000

LOCUS REAL	LOCUS IMAG	DIST TO ORIGIN	GAIN	ZETA	CO
0.	53.935300	60.800000	0.	.00000	1
.12293051	62.377390	62.377501	1.09639	.00197	5
0.	62.734558	62.734558	1.42474	.00000	4
-3.2433092	54.735260	64.536470	7.24999	.05022	0
-5.0330000	62.700000	62.303281	0.	.08033	2

BRANCH NUMBER   10

CALCULATION STEP SIZE =   .8000
PRINTING STEP SIZE   = 4.000

LOCUS REAL	LOCUS IMAG	DIST TO ORIGIN	GAIN	ZETA	CO
0.	-53.300300	60.800000	0.	.00000	1
.12293051	-62.377350	62.377501	1.09639	.00197	5
0.	-62.734558	62.734558	1.42474	.00000	4
-3.2733092	-54.593260	54.536470	7.24999	.05022	0
-5.0330000	-62.700000	62.303231	0.	.08033	2

***********   F1130JJ   //// END OF LIST ////

Appendix B

Root Locus Diagrams and Time Response Plots

Figure B1. Root locus diagrams for base weightings.
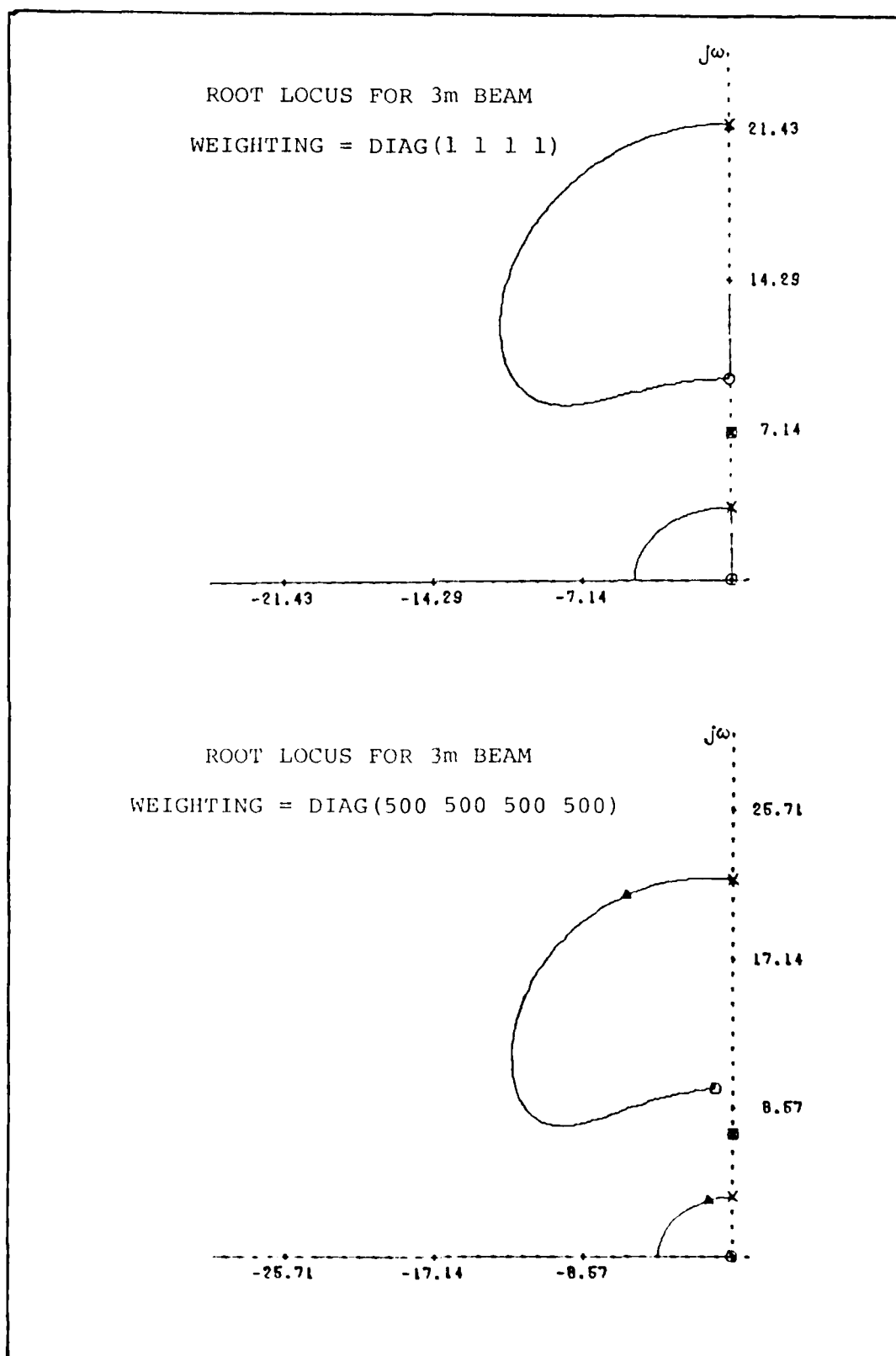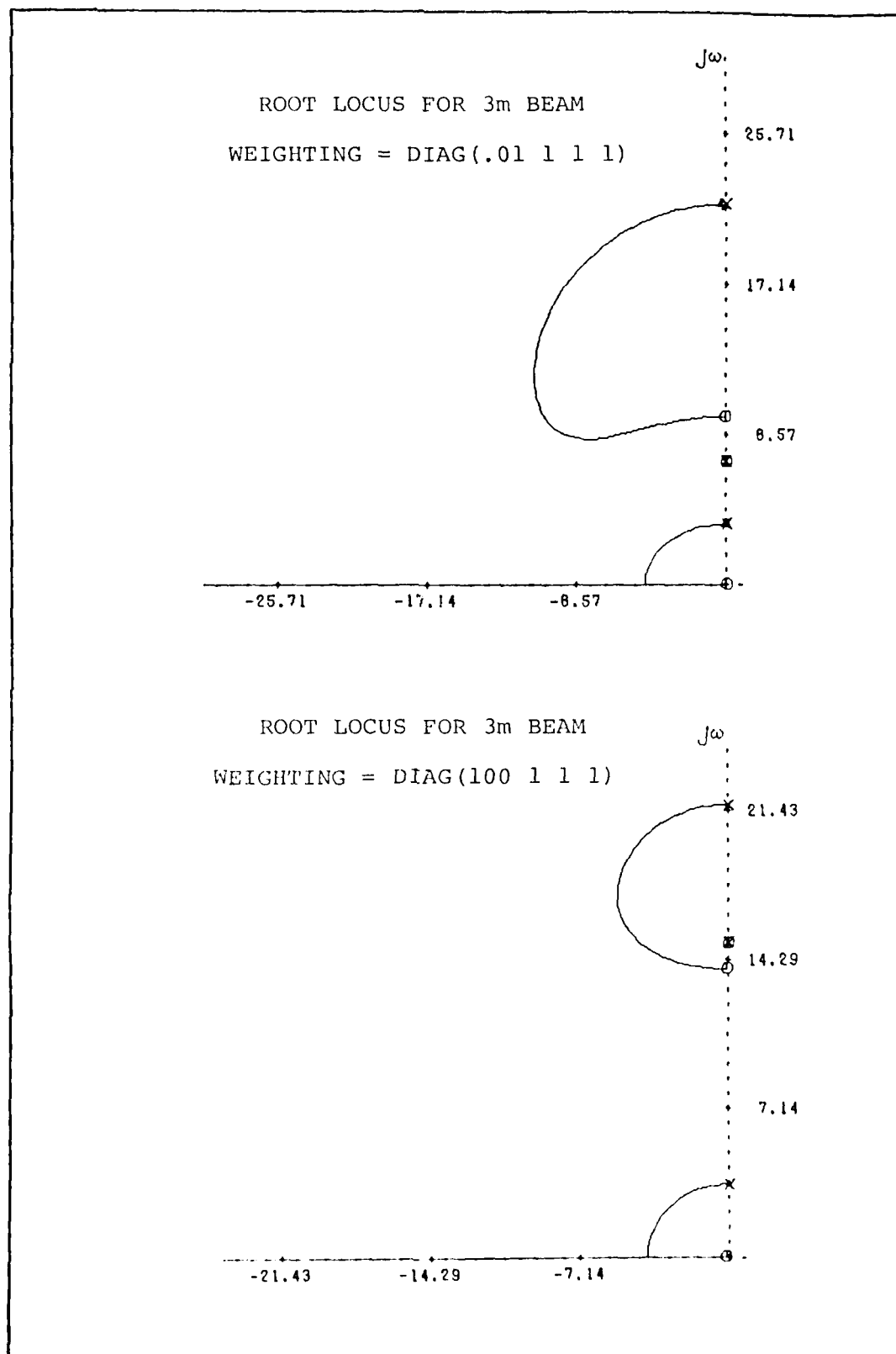
Figure B2. Root locus diagrams for first state weighting variation.

-46-

ROOT LOCUS FOR 3m BEAM

WEIGHTING = DIAG(1 .01 1 1)

ROOT LOCUS FOR 3m BEAM

WEIGHTING = DIAG(1 100 1 1)
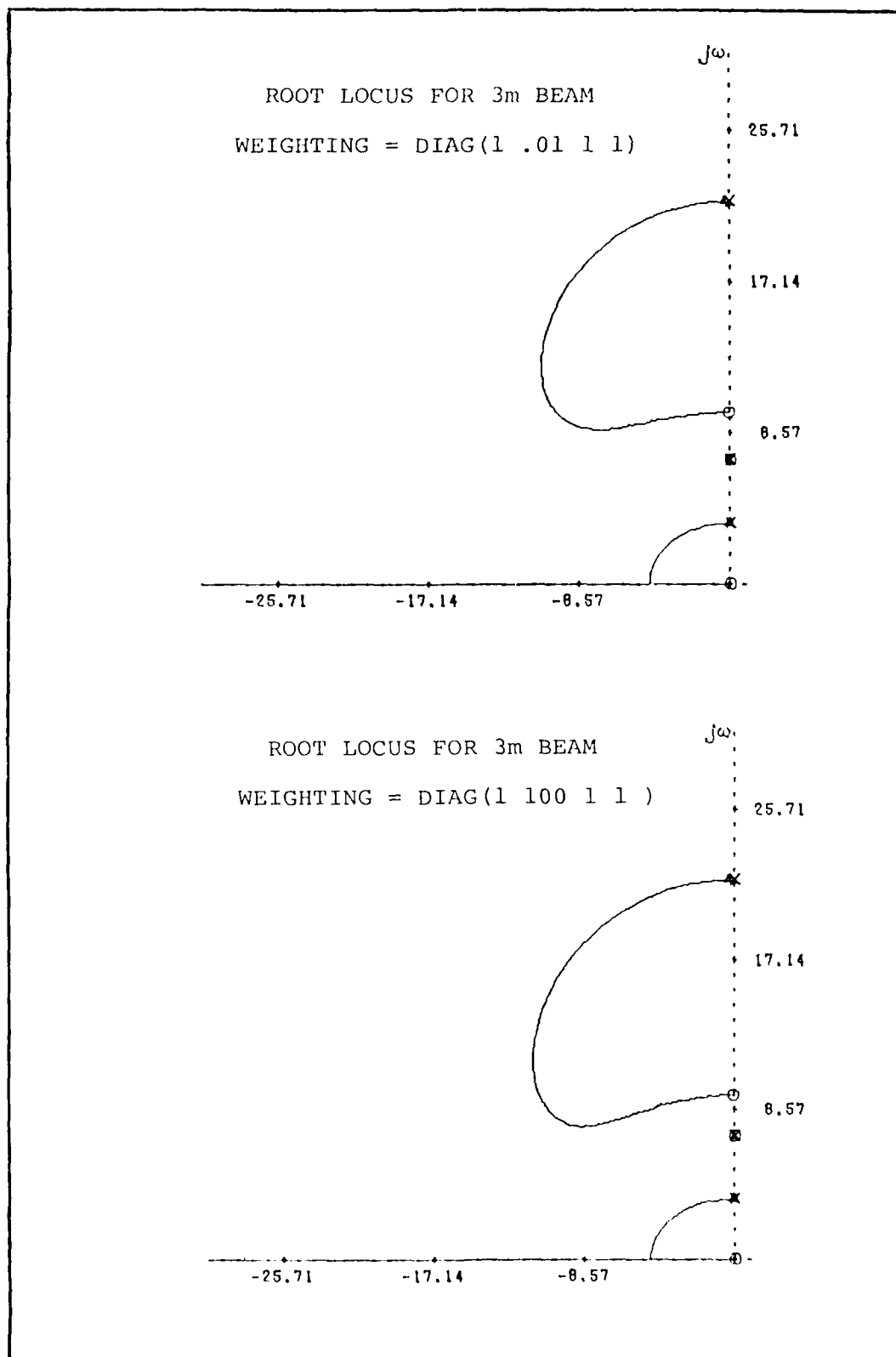
Figure B3. Root locus diagrams for second state weighting variation.

ROOT LOCUS FOR 3m BEAM

WEIGHTING = DIAG(1 1 .01 1)

ROOT LOCUS FOR 3m BEAM

WEIGHTING = DIAG(1 1 100 1)
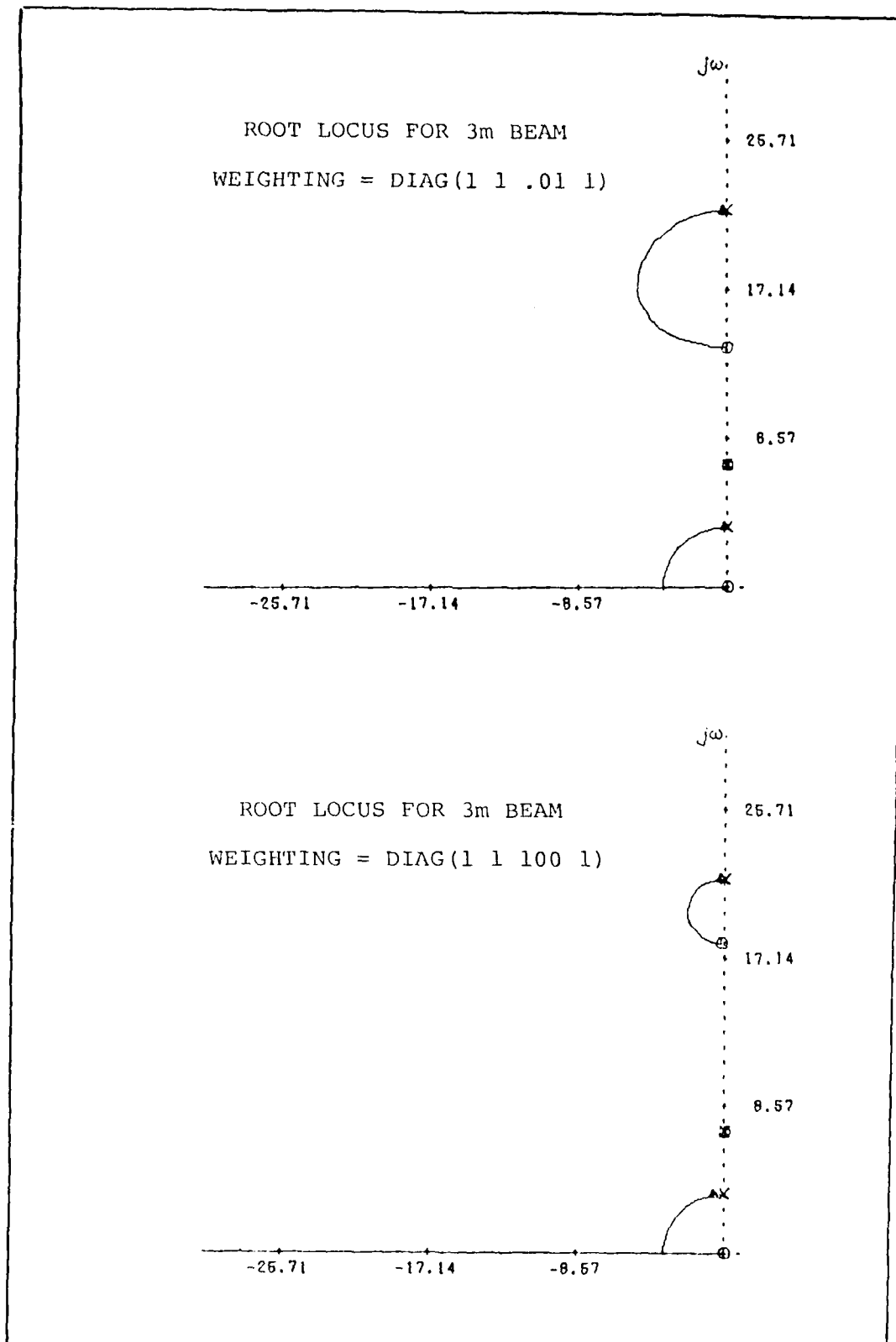
Figure B4.   Root locus diagrams for third state weighting variation.

-48-
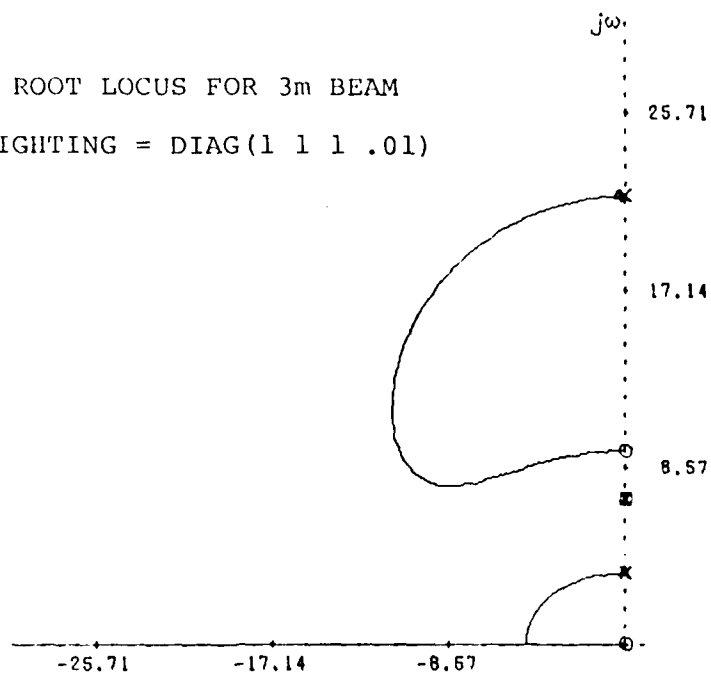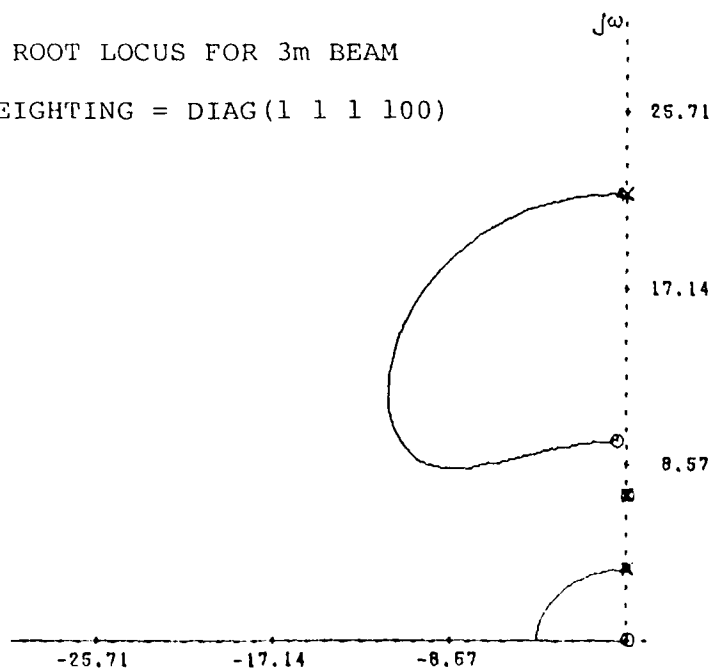
Figure B5. Root locus diagrams for fourth state weighting variatio
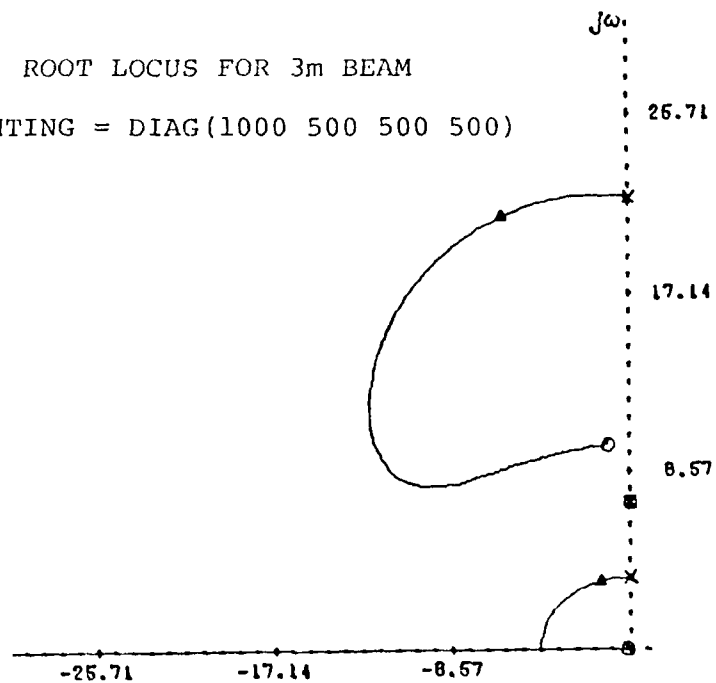
Figure B6. Root locus diagrams for first state weighting variation.
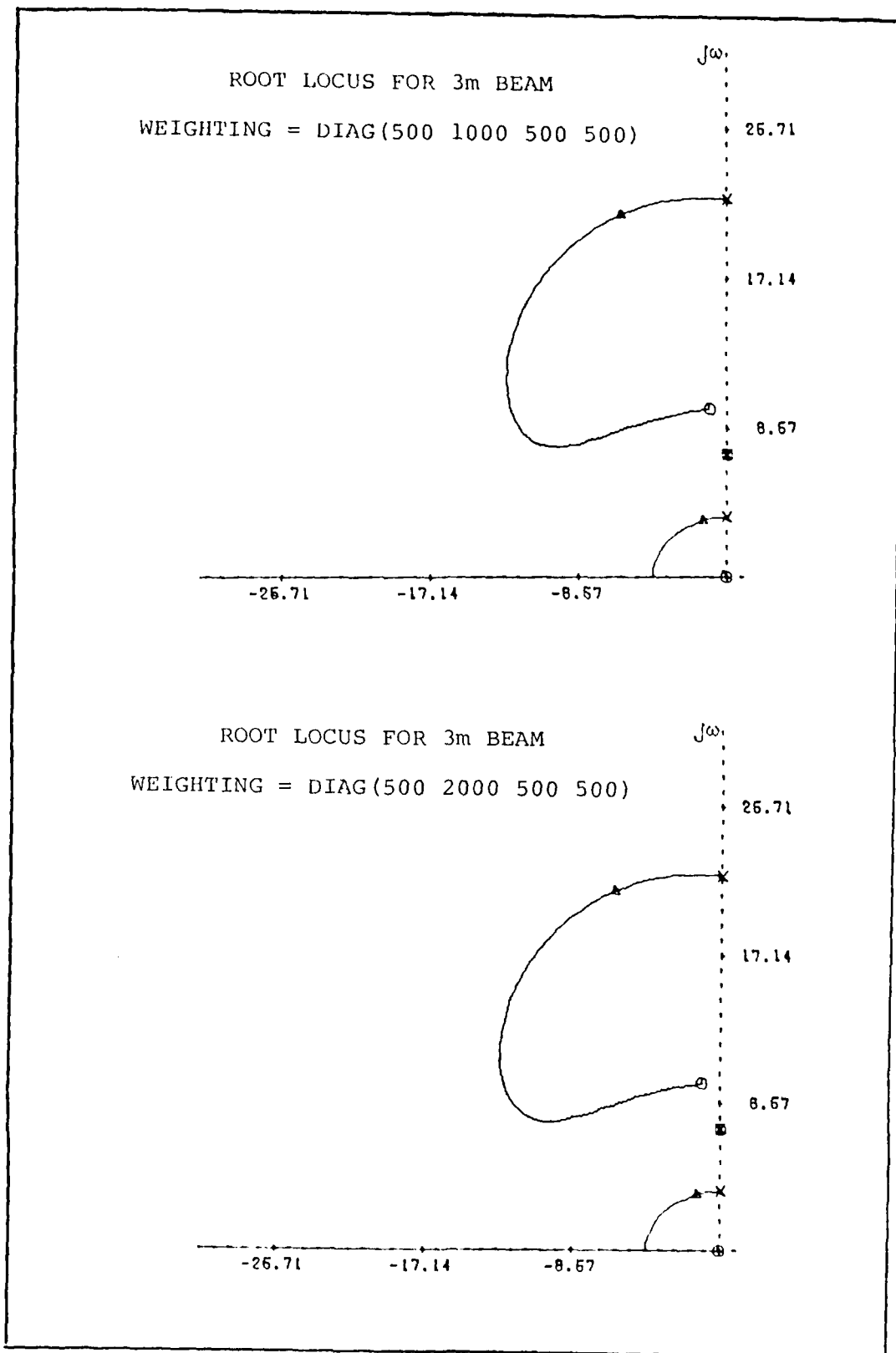
Figure B7. Root locus diagrams for second state weighting variation.

ROOT LOCUS FOR 3m BEAM

WEIGHTING = DIAG(500 500 1000 500)

ROOT LOCUS FOR 3m BEAM

WEIGHTING = DIAG(500 500 2000 500)
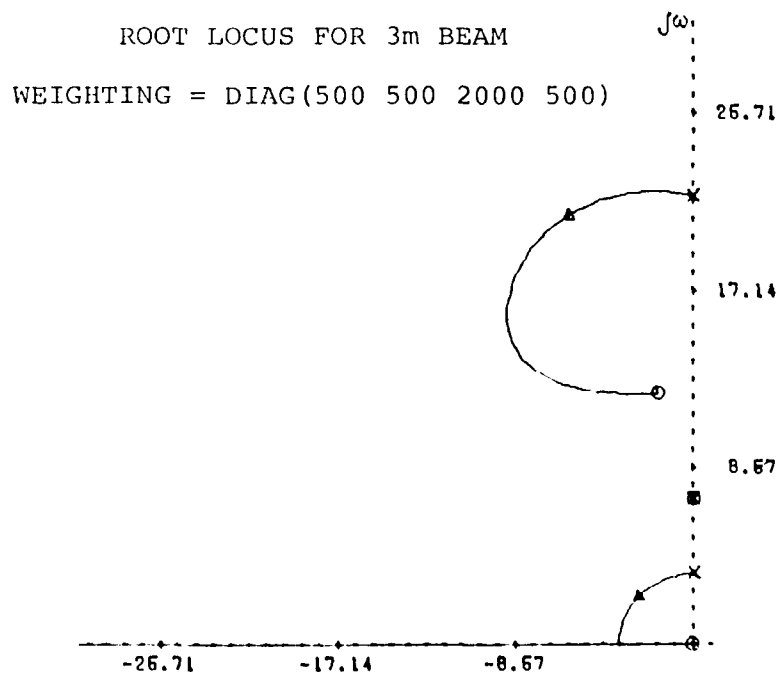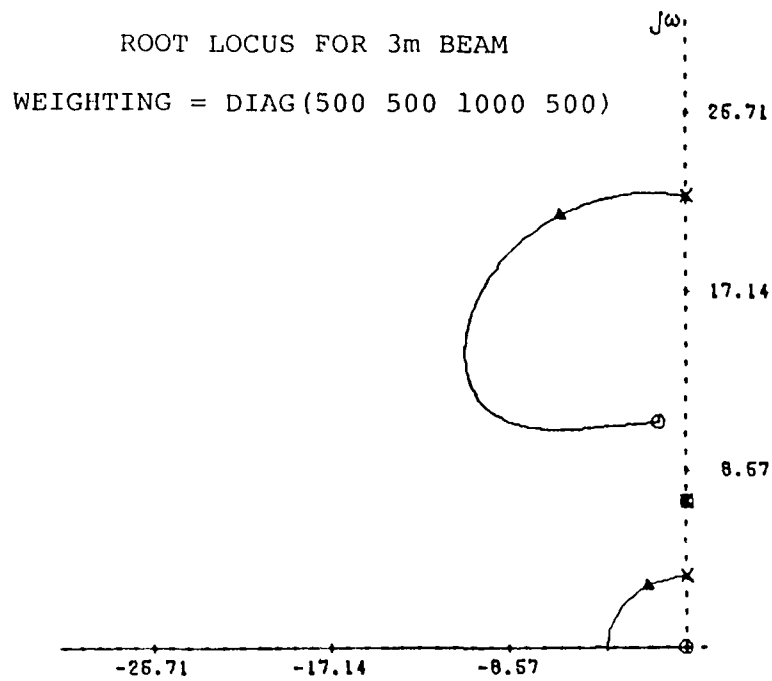
Figure B8. Root locus diagrams for third state weighting variation.

ROOT LOCUS FOR 3m BEAM

WEIGHTING = DIAG(500 500 500 2000)

ROOT LOCUS FOR 3m BEAM

INCLUDING OBSERVER AND RESIDUAL MODE

WEIGHTING = DIAG(500 500 500 2000)
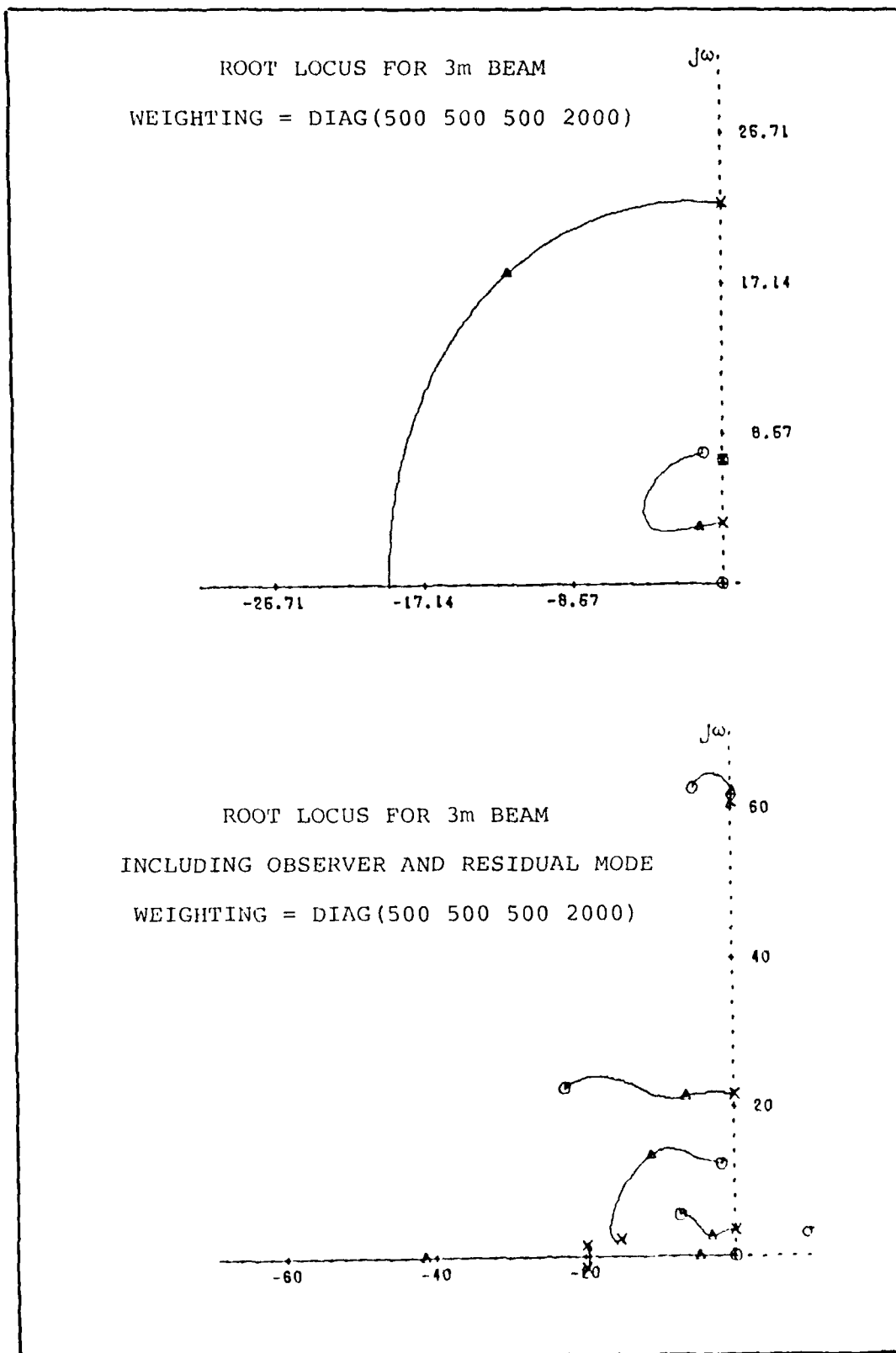
Figure B9. Root locus diagrams for fourth state weighting variation.

ROOT LOCUS FOR 3m BEAM

WEIGHTING = DIAG(100,000 500 500 500)
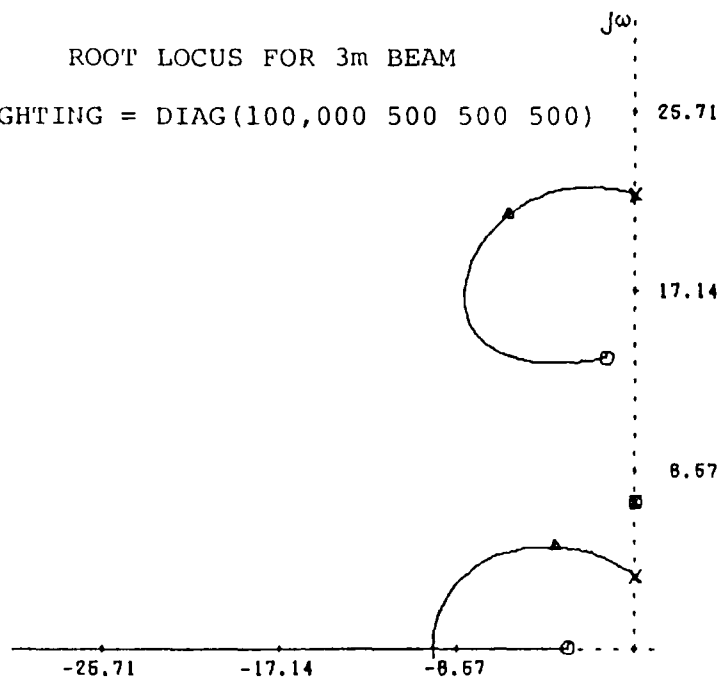
ROOT LOCUS FOR 3m BEAM

WEIGHTING = DIAG(500 10,000 500 500)
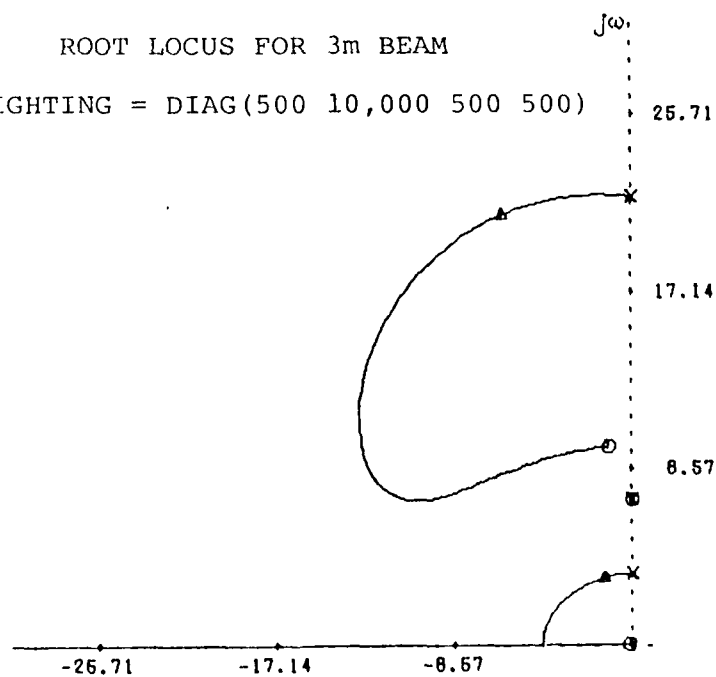
Figure B10.   Root locus diagrams for large first two state weightings.

-54-
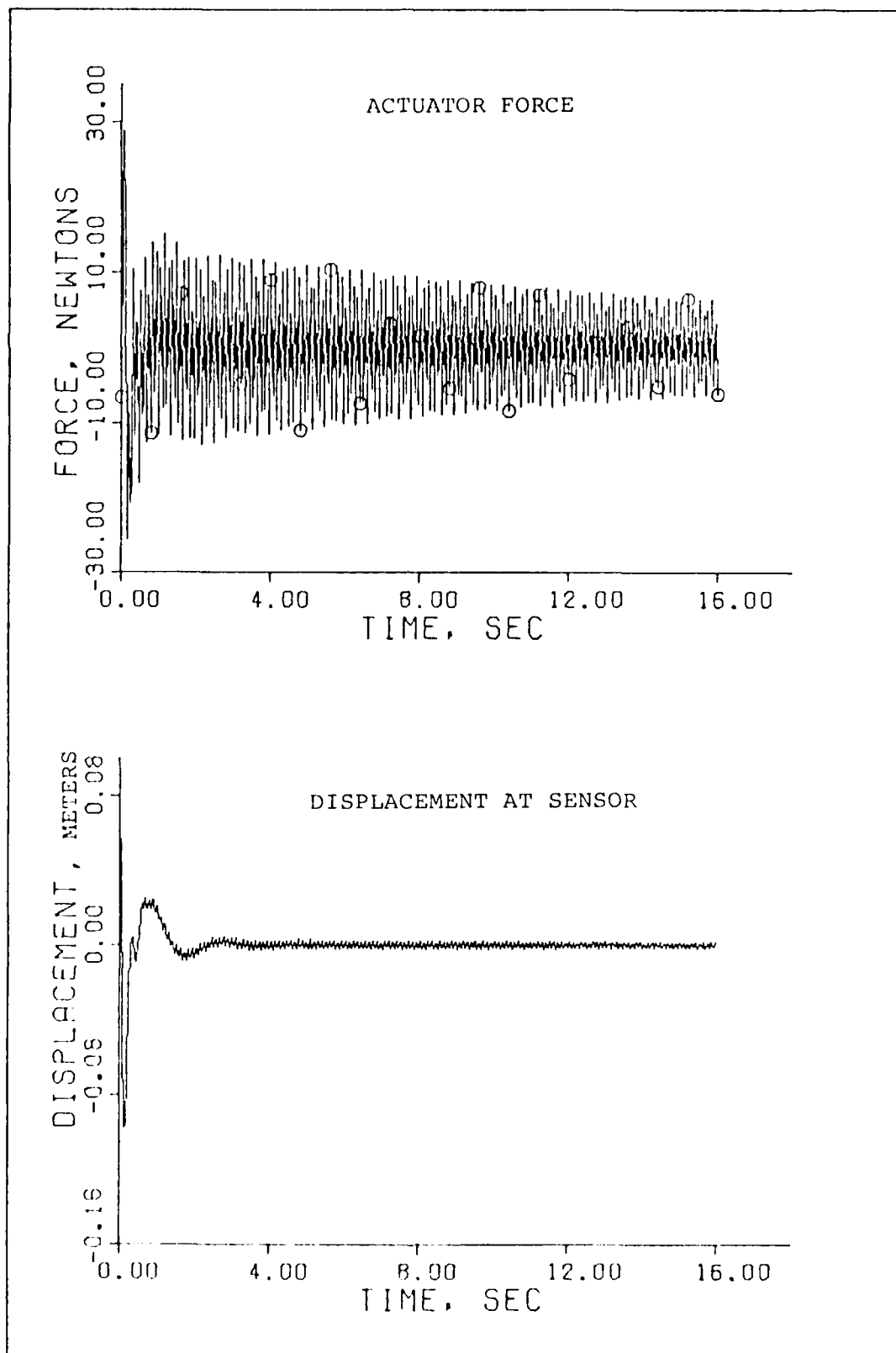
Figure B11. Time response for weighting = DIAG(500 500 500 500).
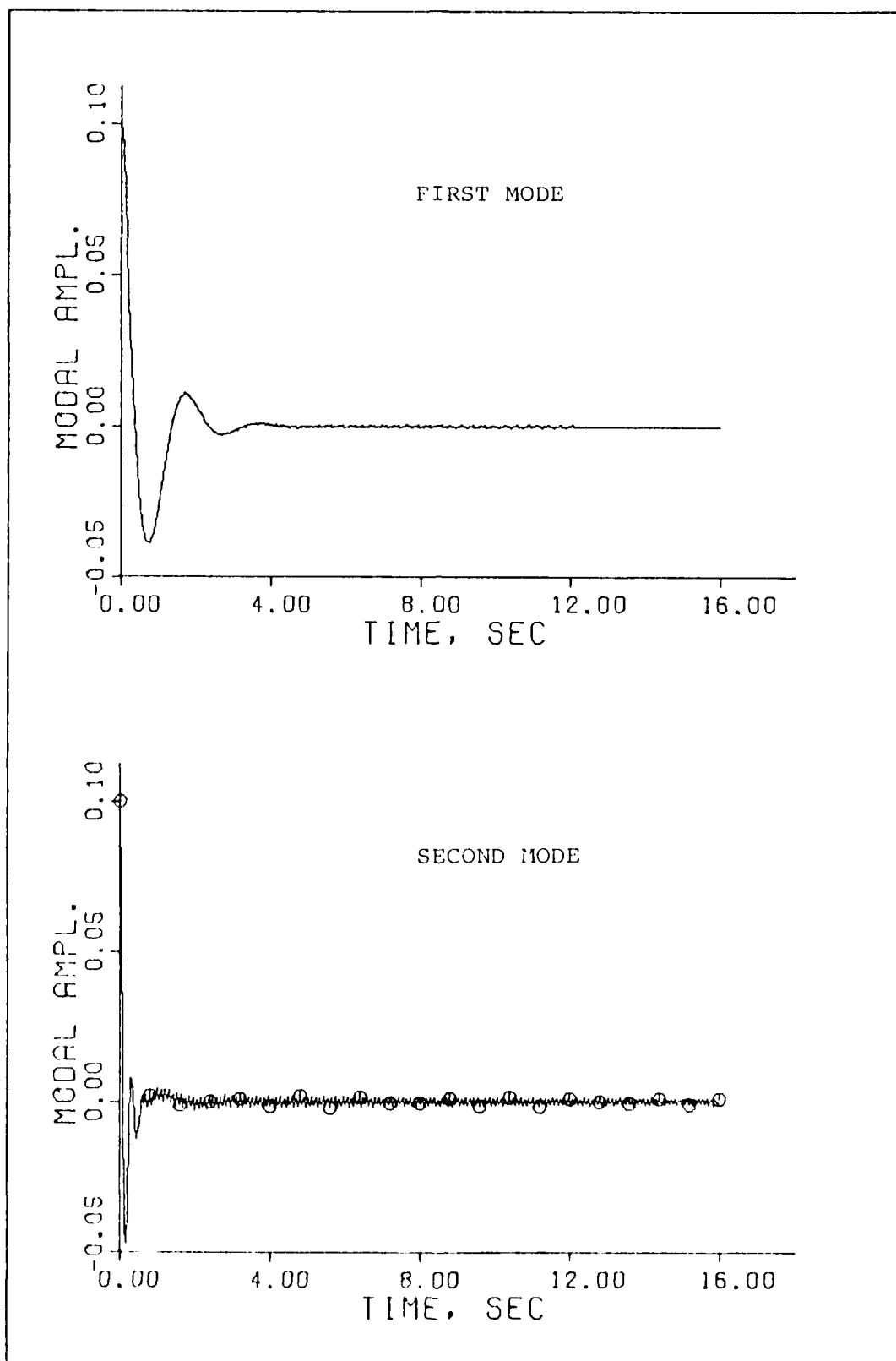
Figure B12.   Time response for weighting = DIAG(500 500 500 500).
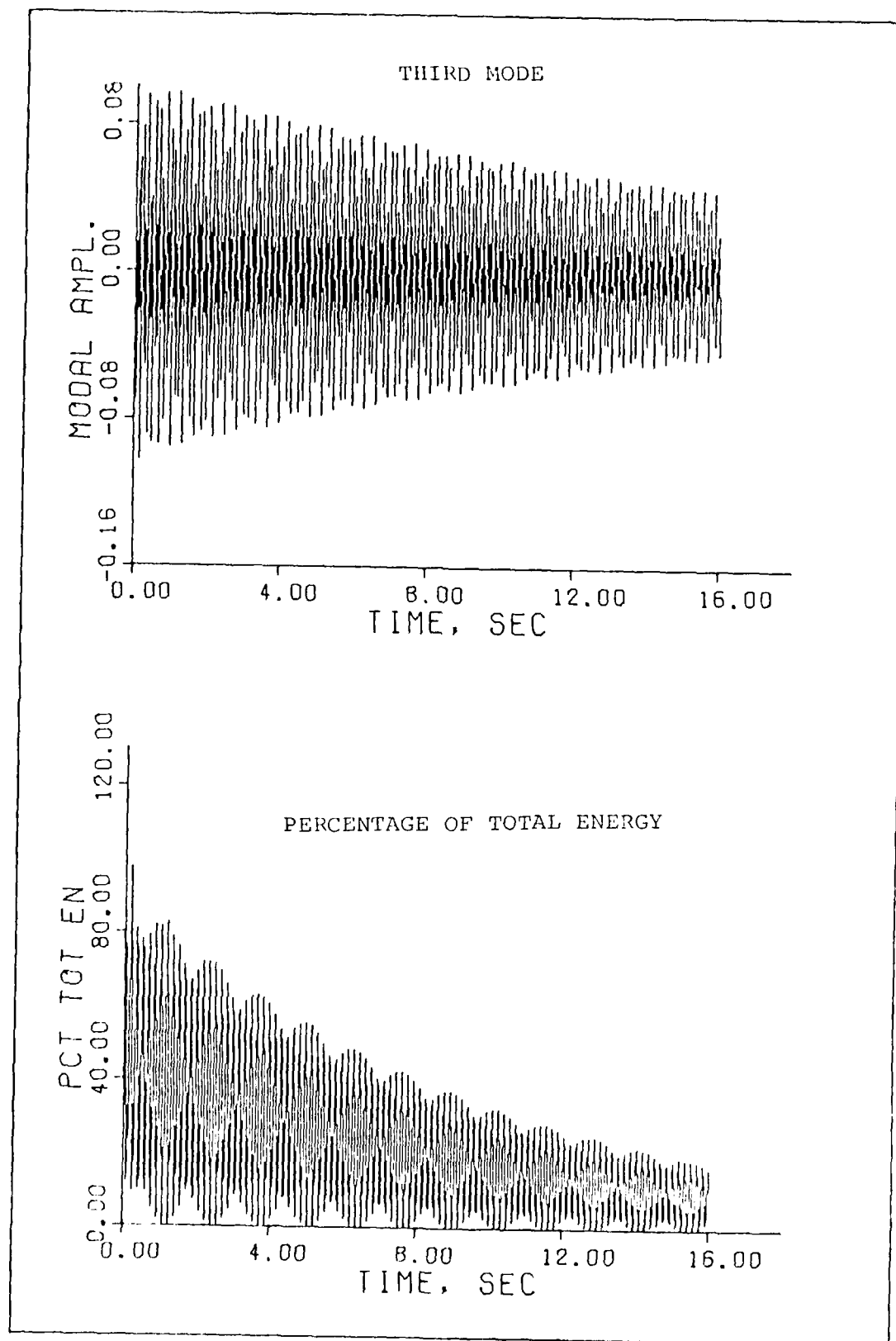
Figure B13. Time response for weighting = DIAG(500 500 500 500).
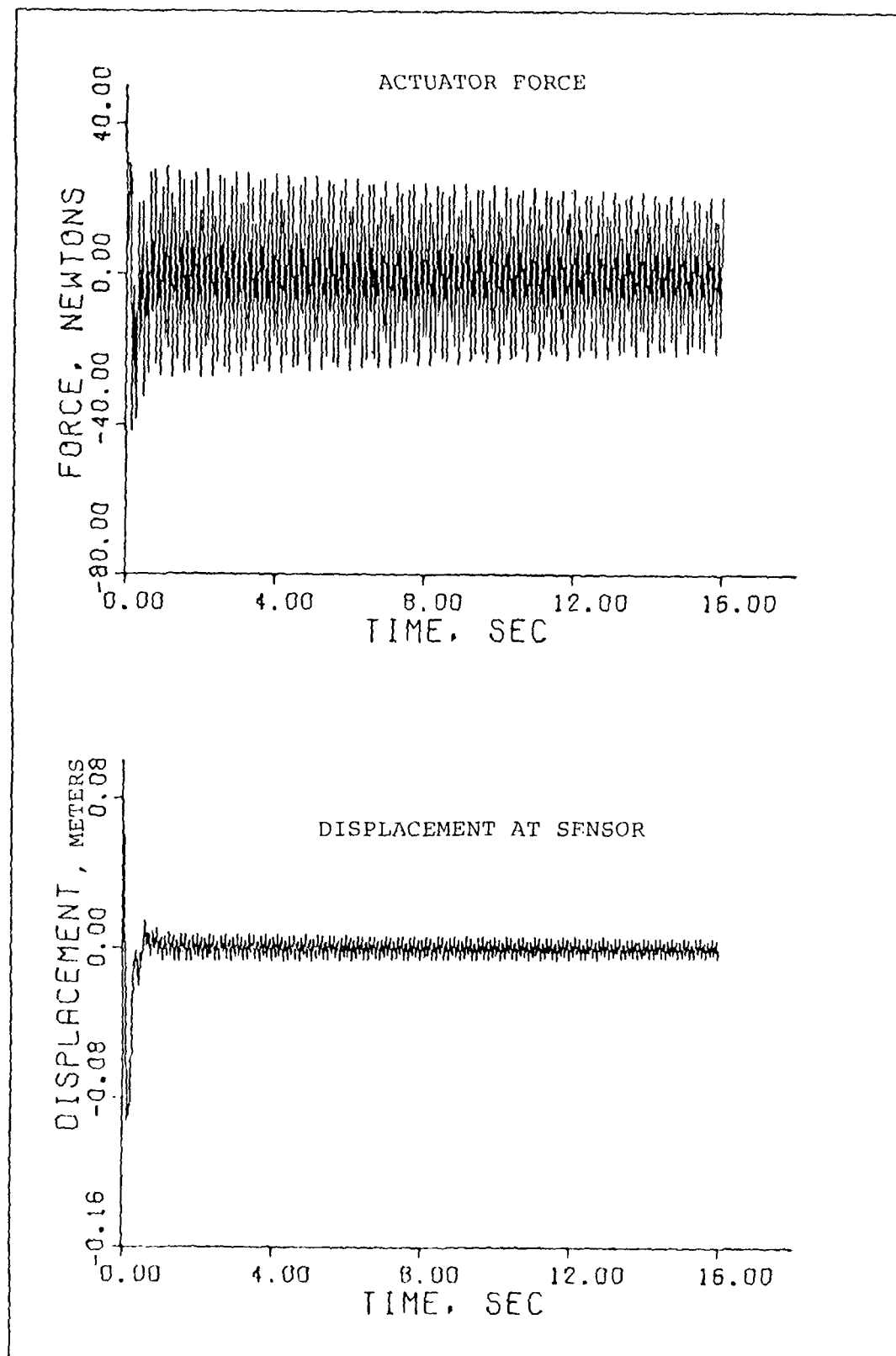
Figure B14. Time response for weighting = DIAG(100,000 500 500 500).
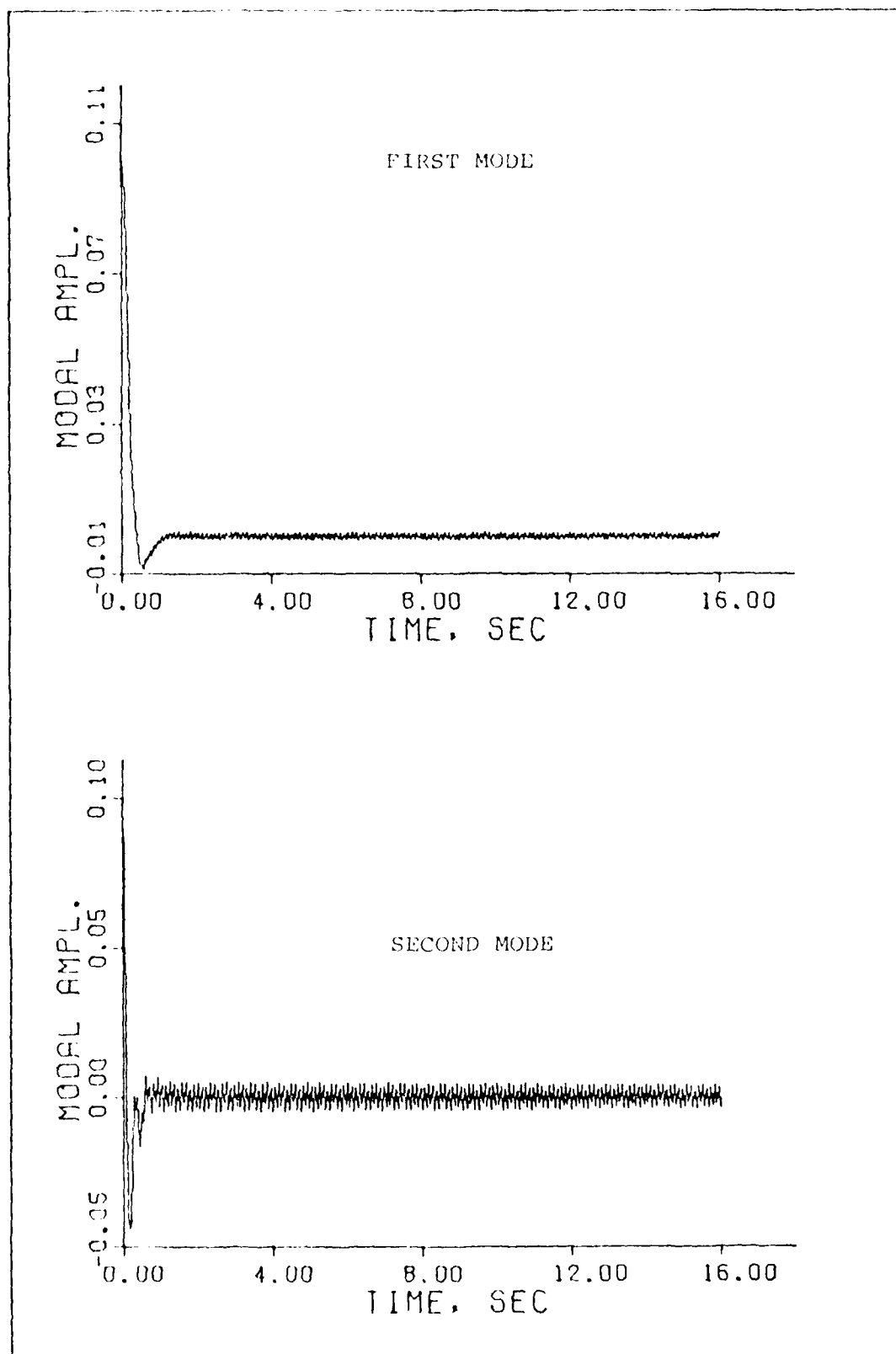
Figure B15. Time response for weighting = DIAG(100,000 500 500 500).
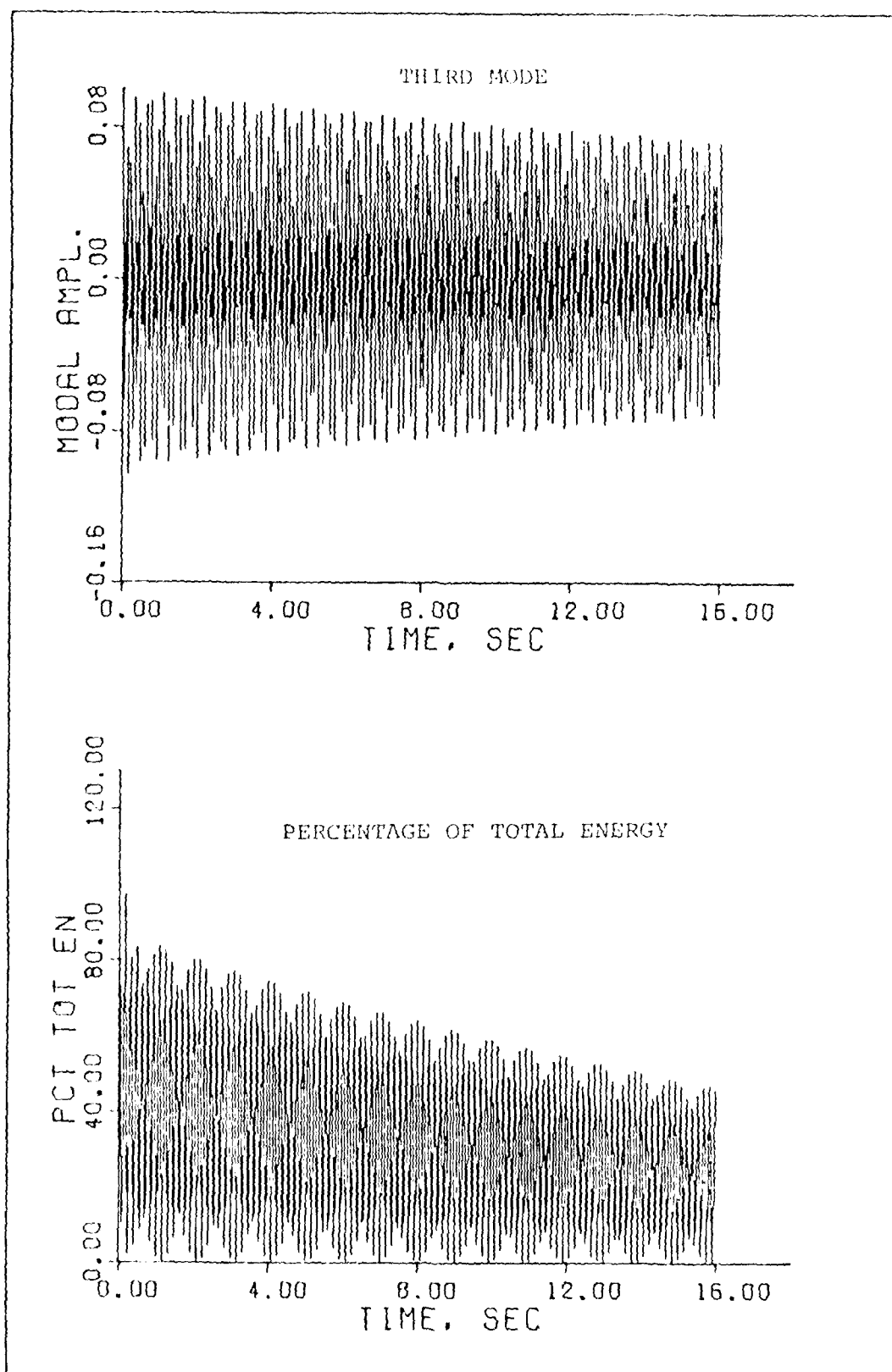
Figure B16. Time response for weighting = DIAG(100,000 500 500 500).
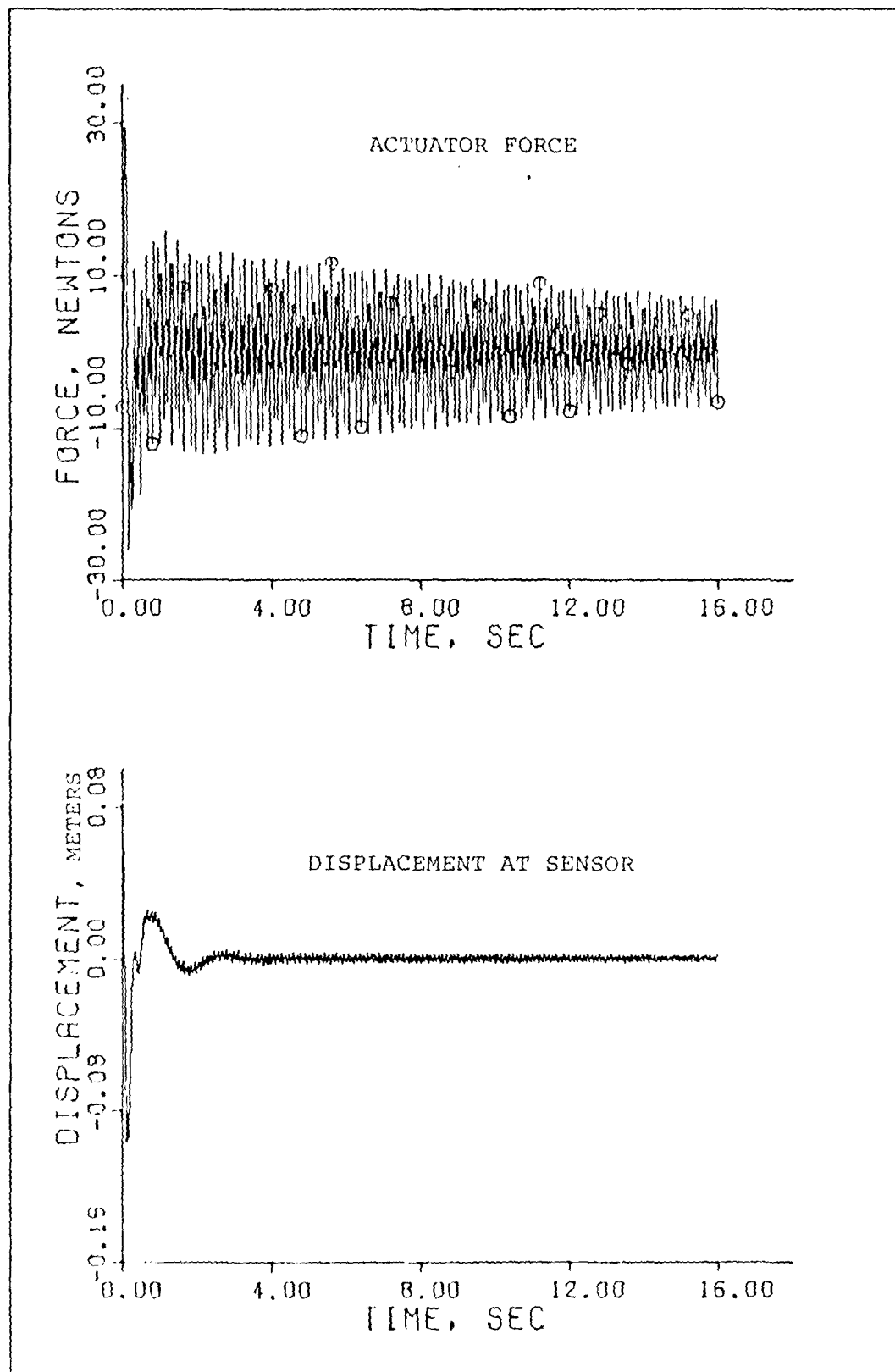
Figure B17.   Time response for weighting = DIAG(500 10,000 500 500).
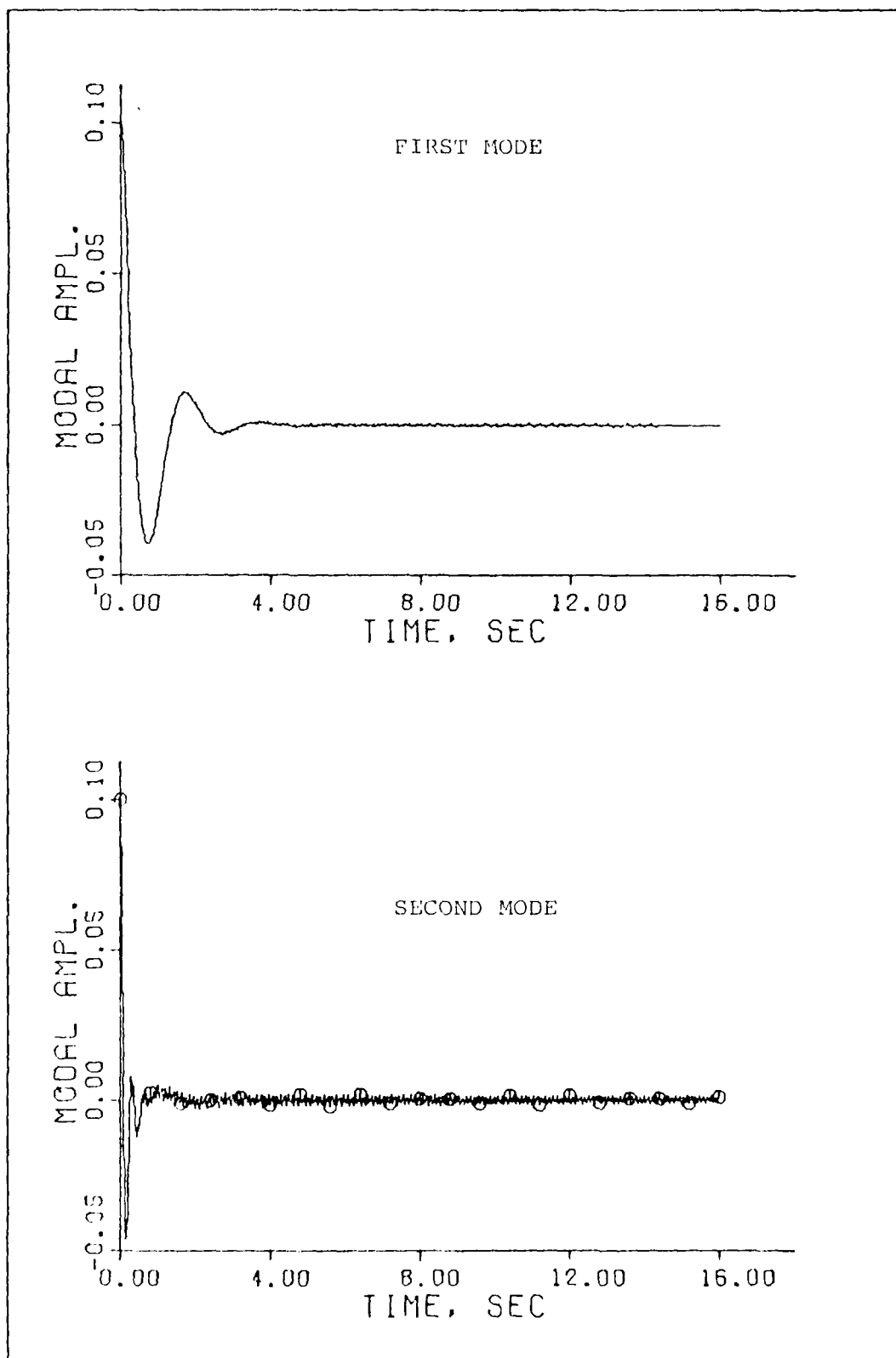
Figure B18.   Time response for weighting = DIAG(500 10,000 500 500).
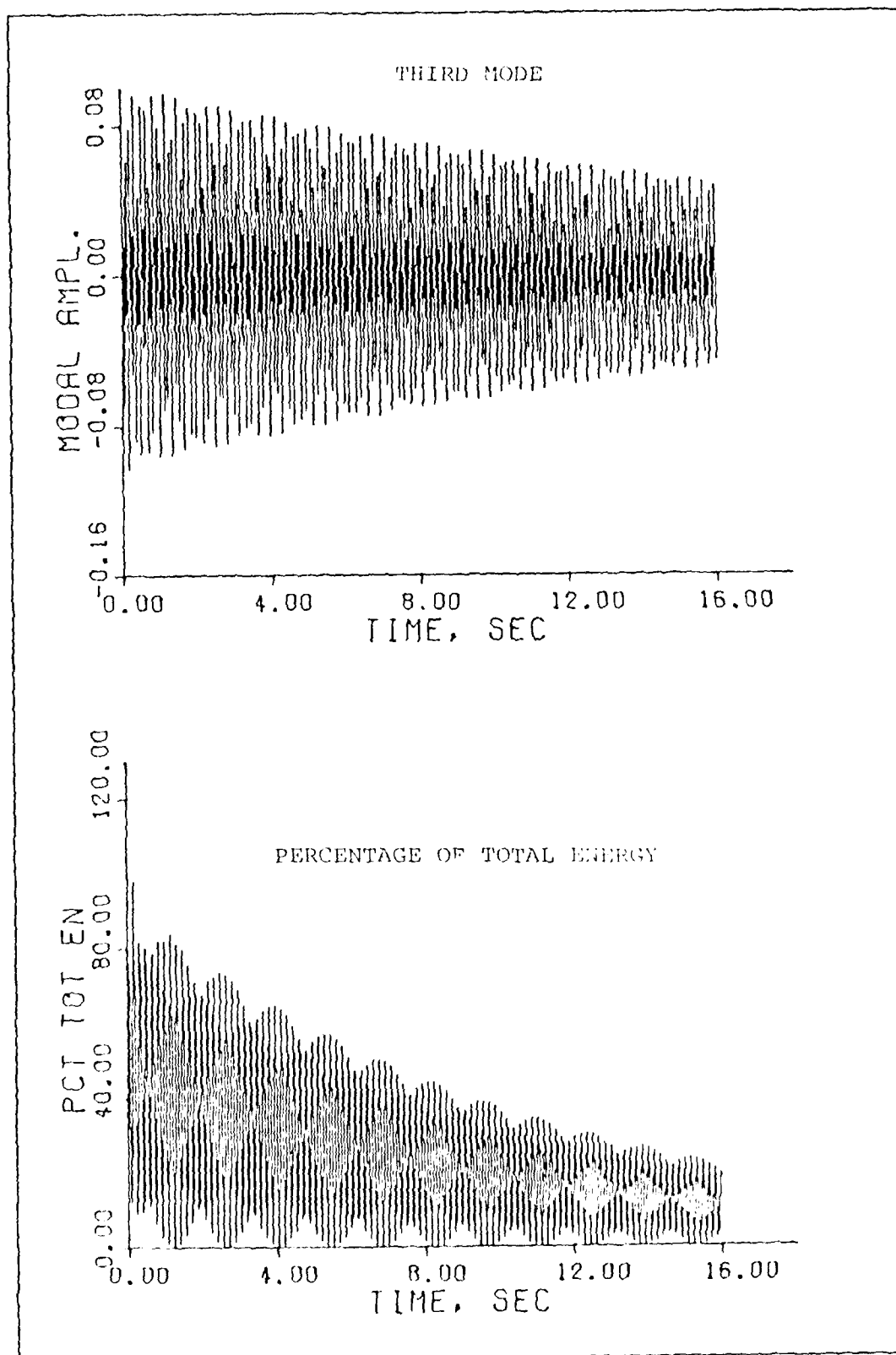
Figure B19. Time response for weighting = DIAG(500 10,000 500 500).
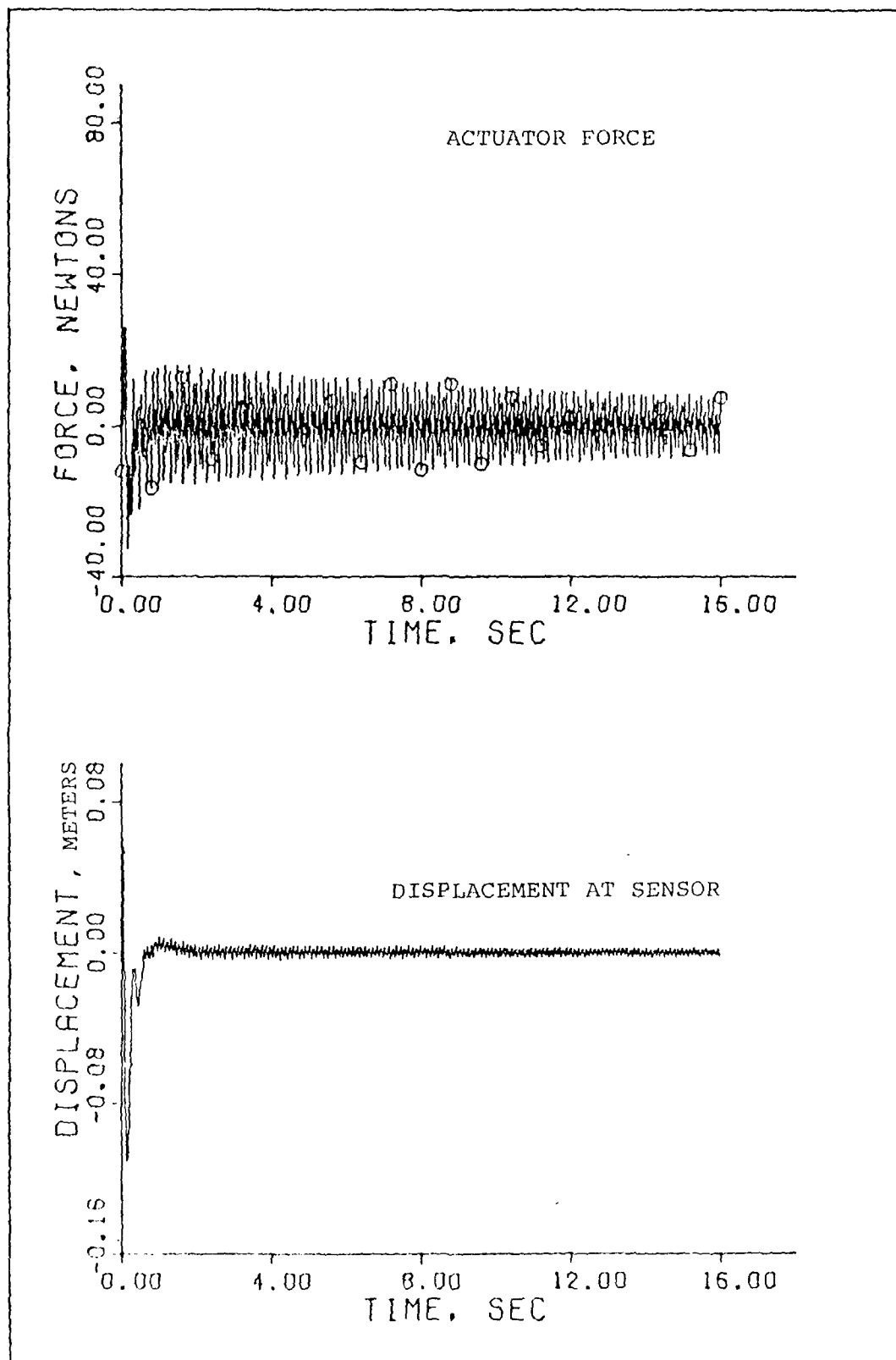
Figure B20. Time response for weighting = DIAG(500 500 2000 500).
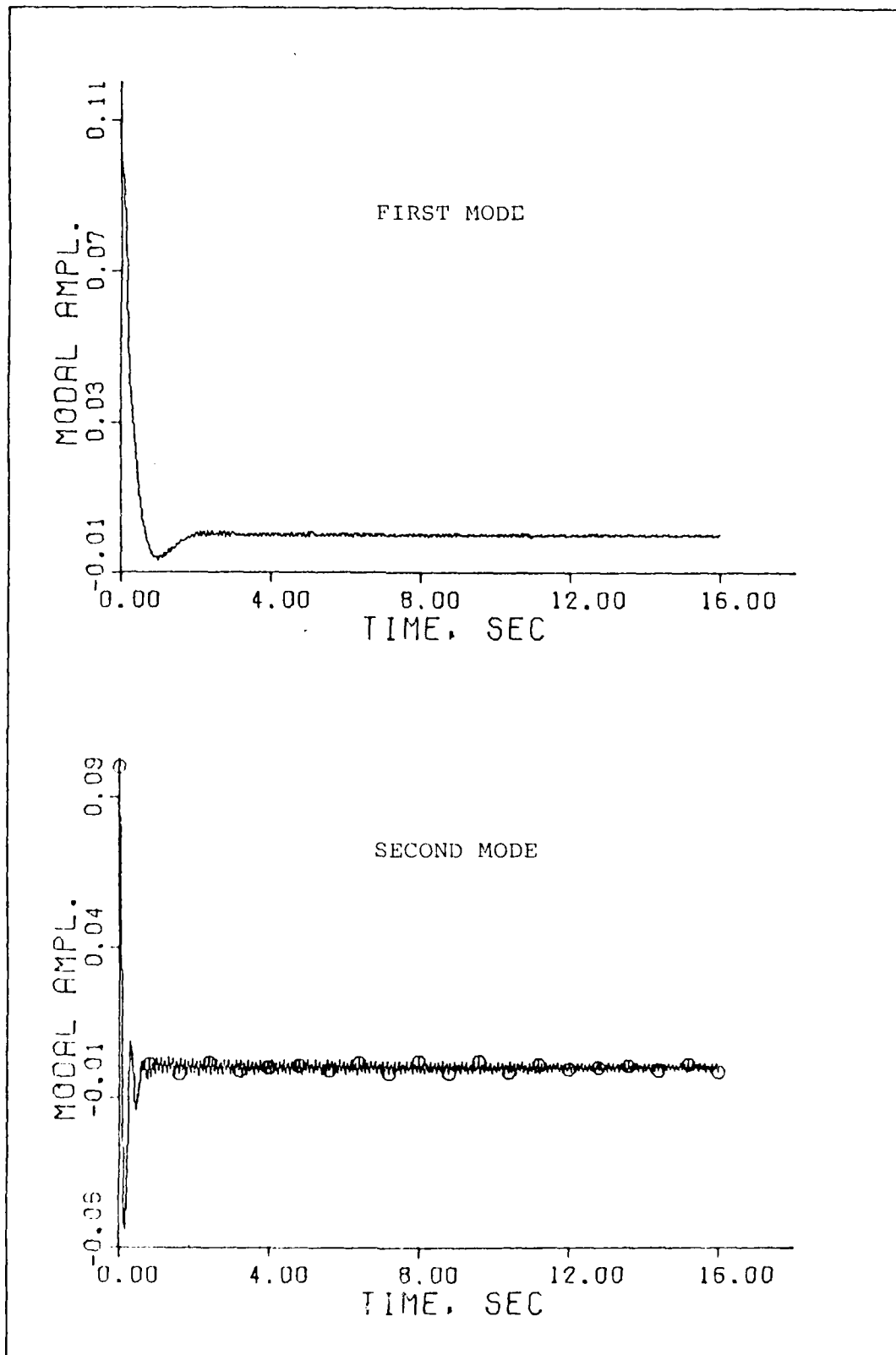
Figure B21.   Time response for weighting = DIAG(500 500 2000 500).
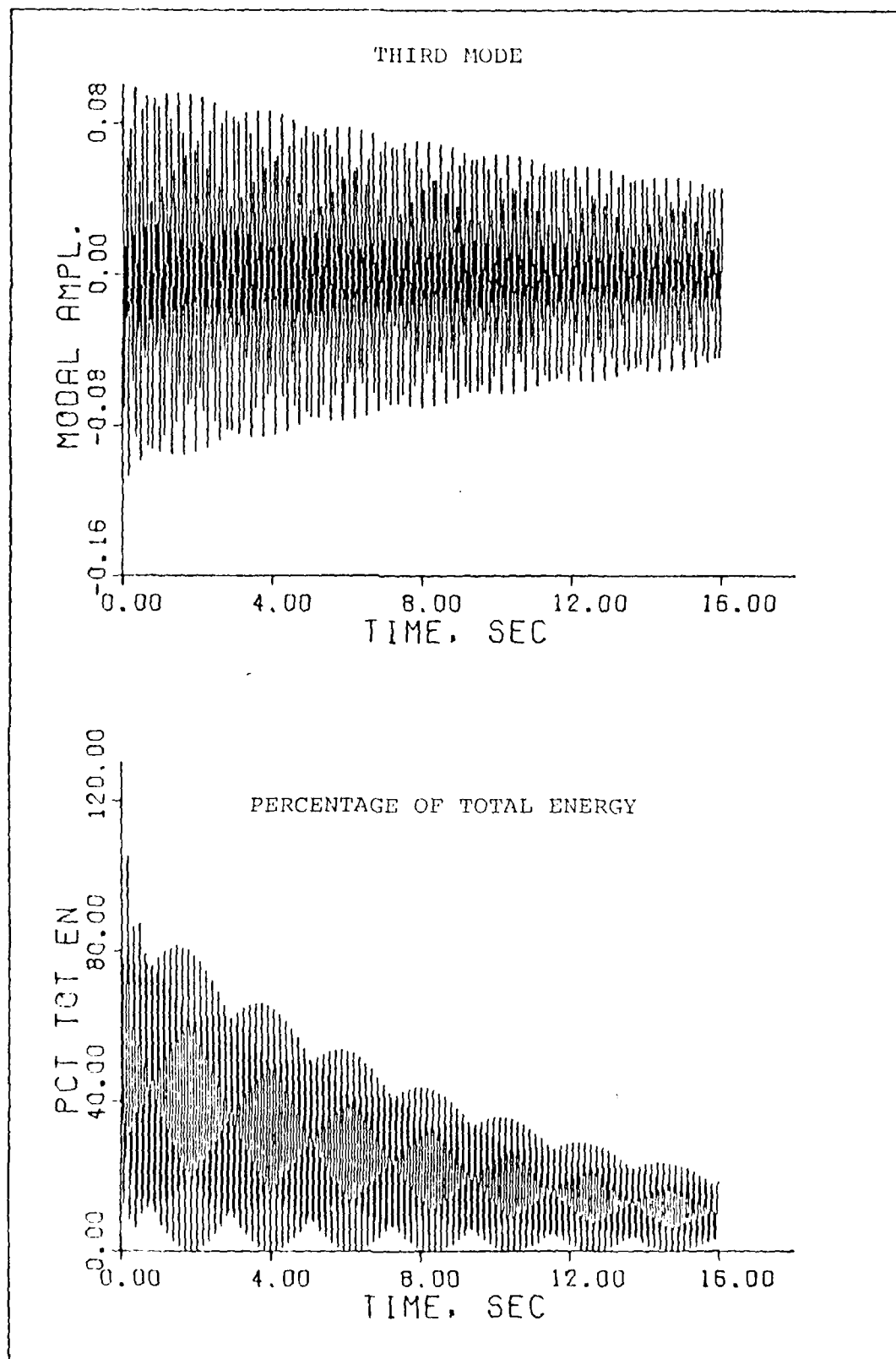
Figure B22.   Time response for weighting = DIAG(500 500 2000 500).
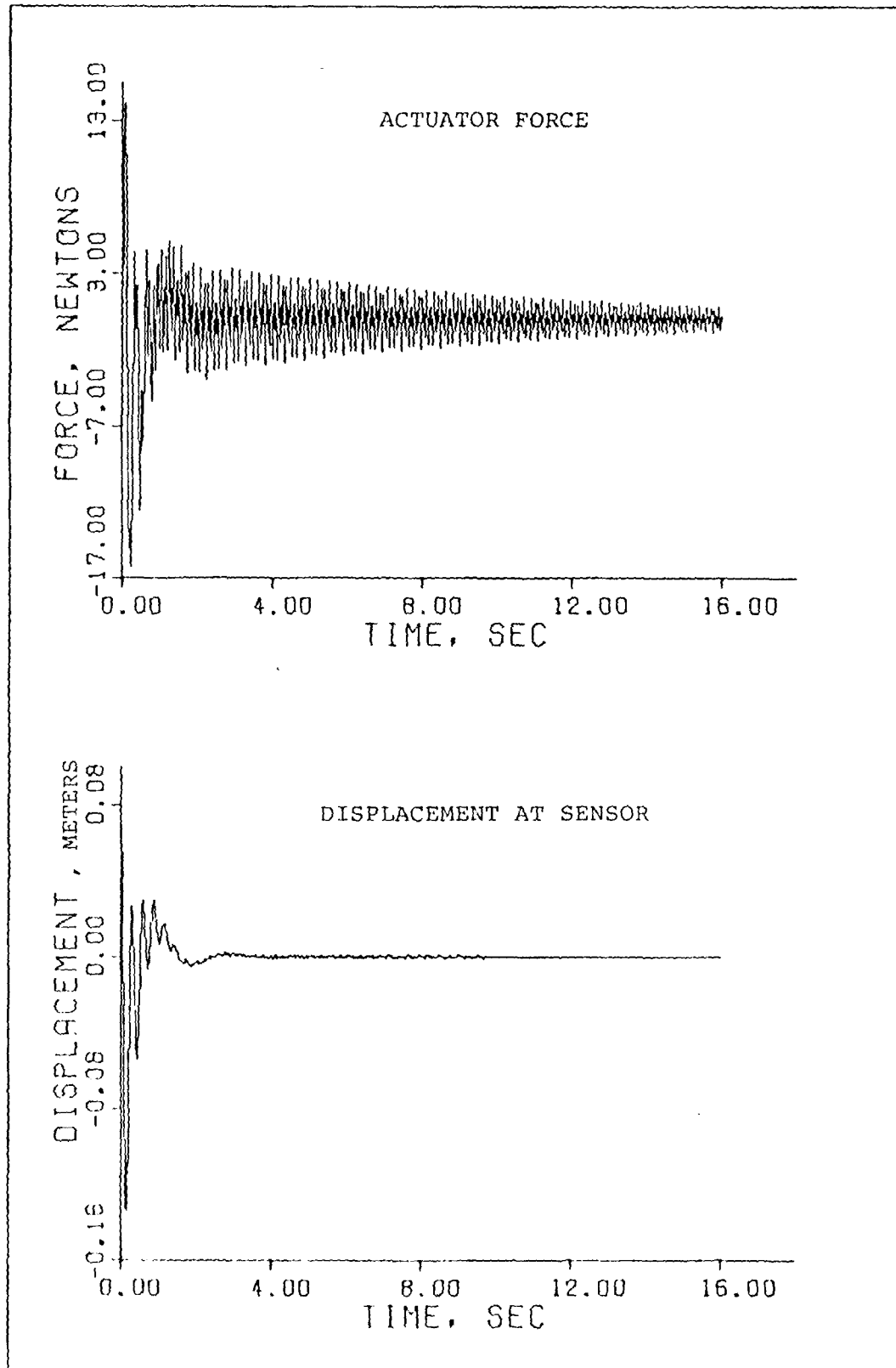
Figure B23. Time response for weighting = DIAG(500 500 500 100).
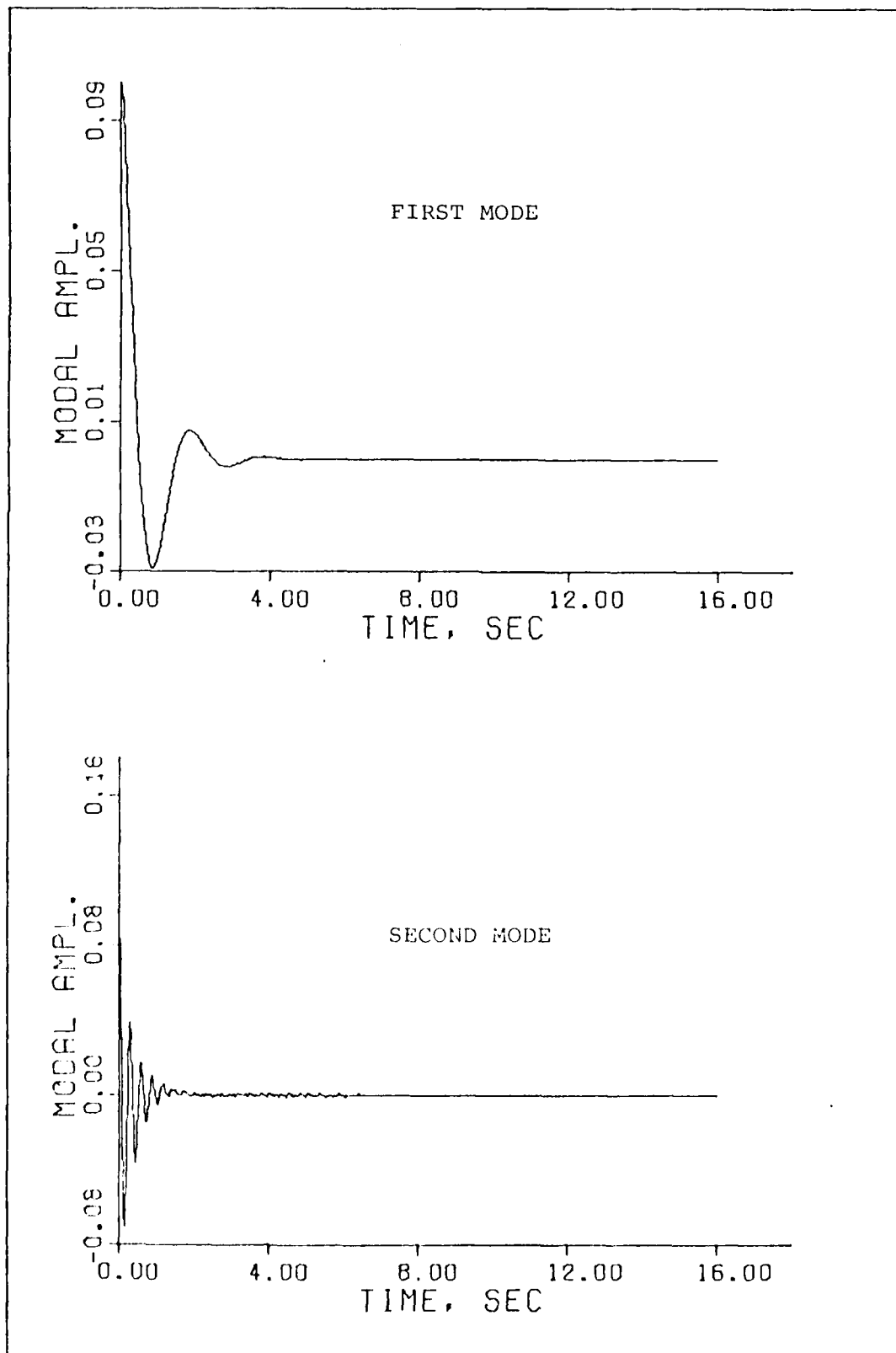
Figure B24. Time response for weighting = DIAG(500 500 500 100)
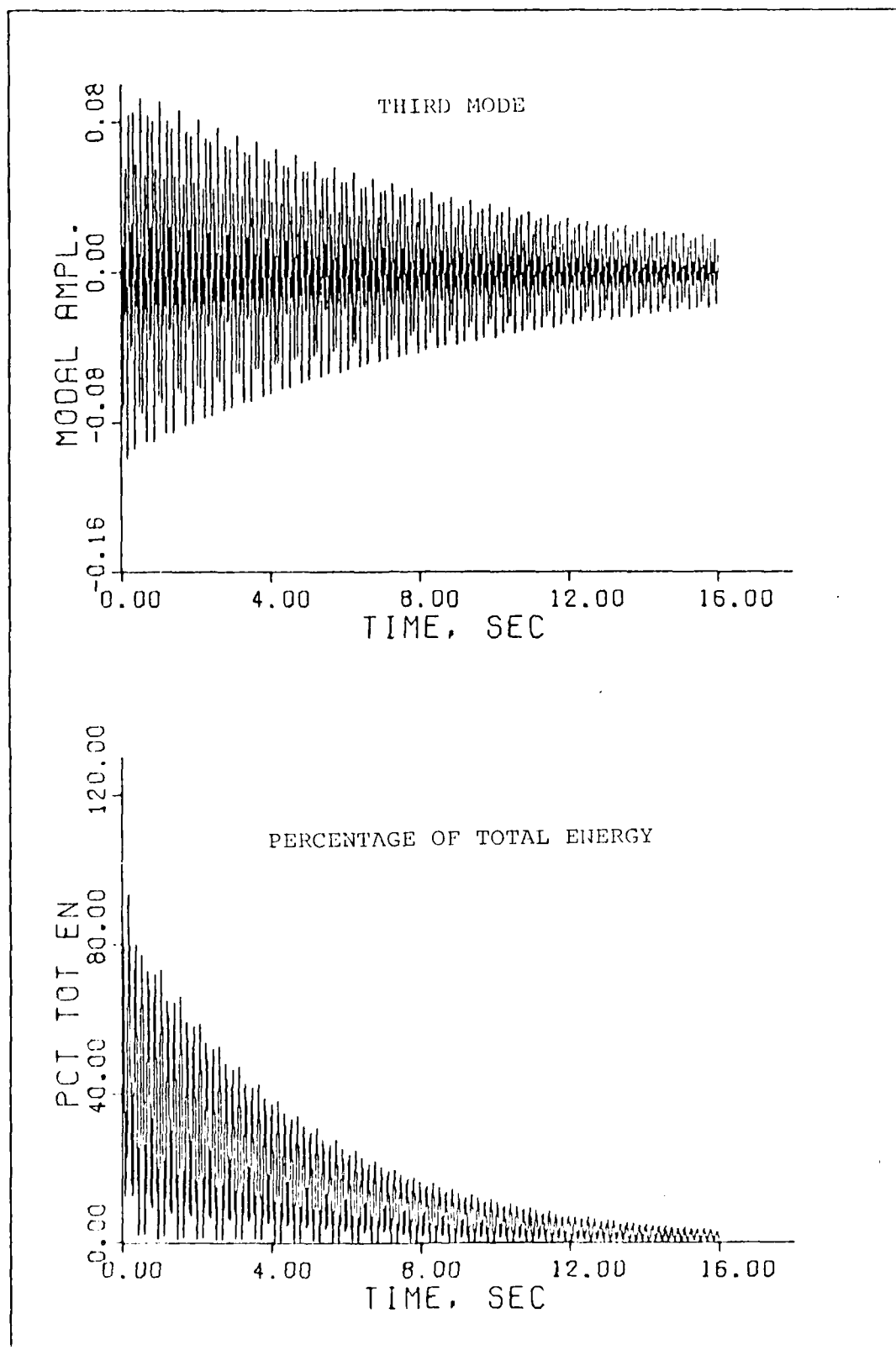
Figure B25. Time response for weighting = DIAG(500 500 500 100)
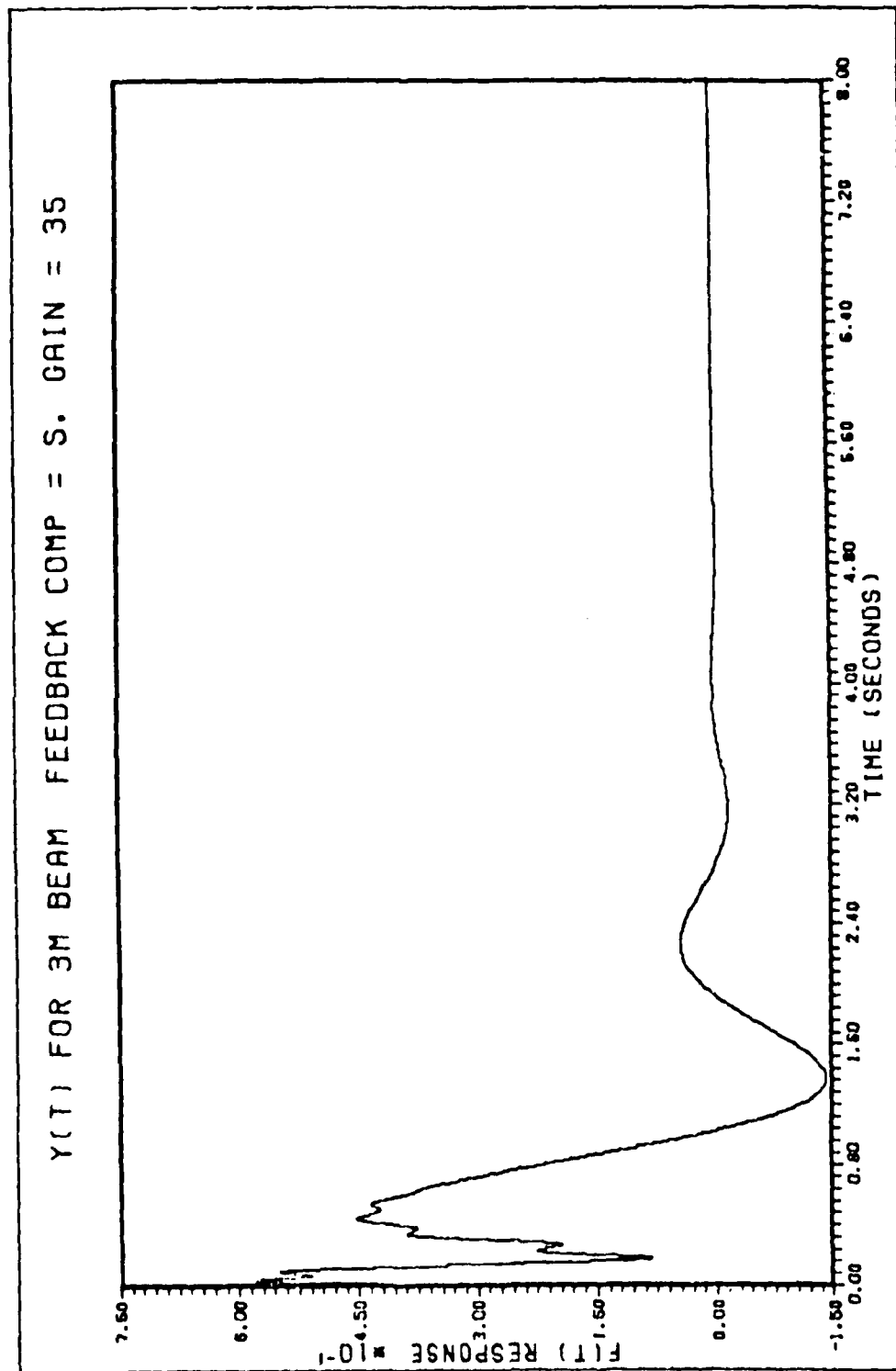
Fig B26.   Sensor displacement for one zero at origin.
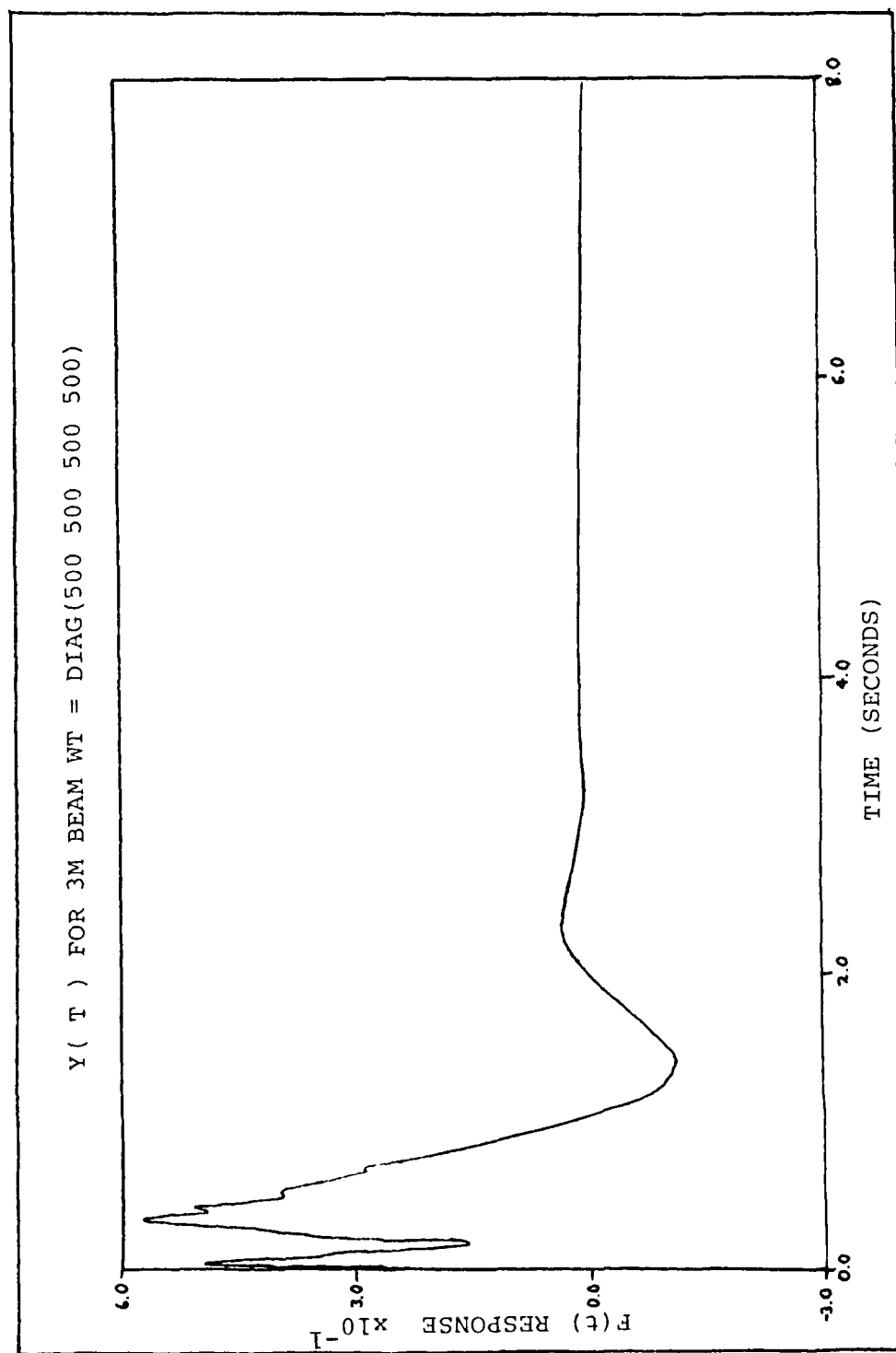
Fig B27. Sensor displacement for optimal regulator with base weighting.

-71-
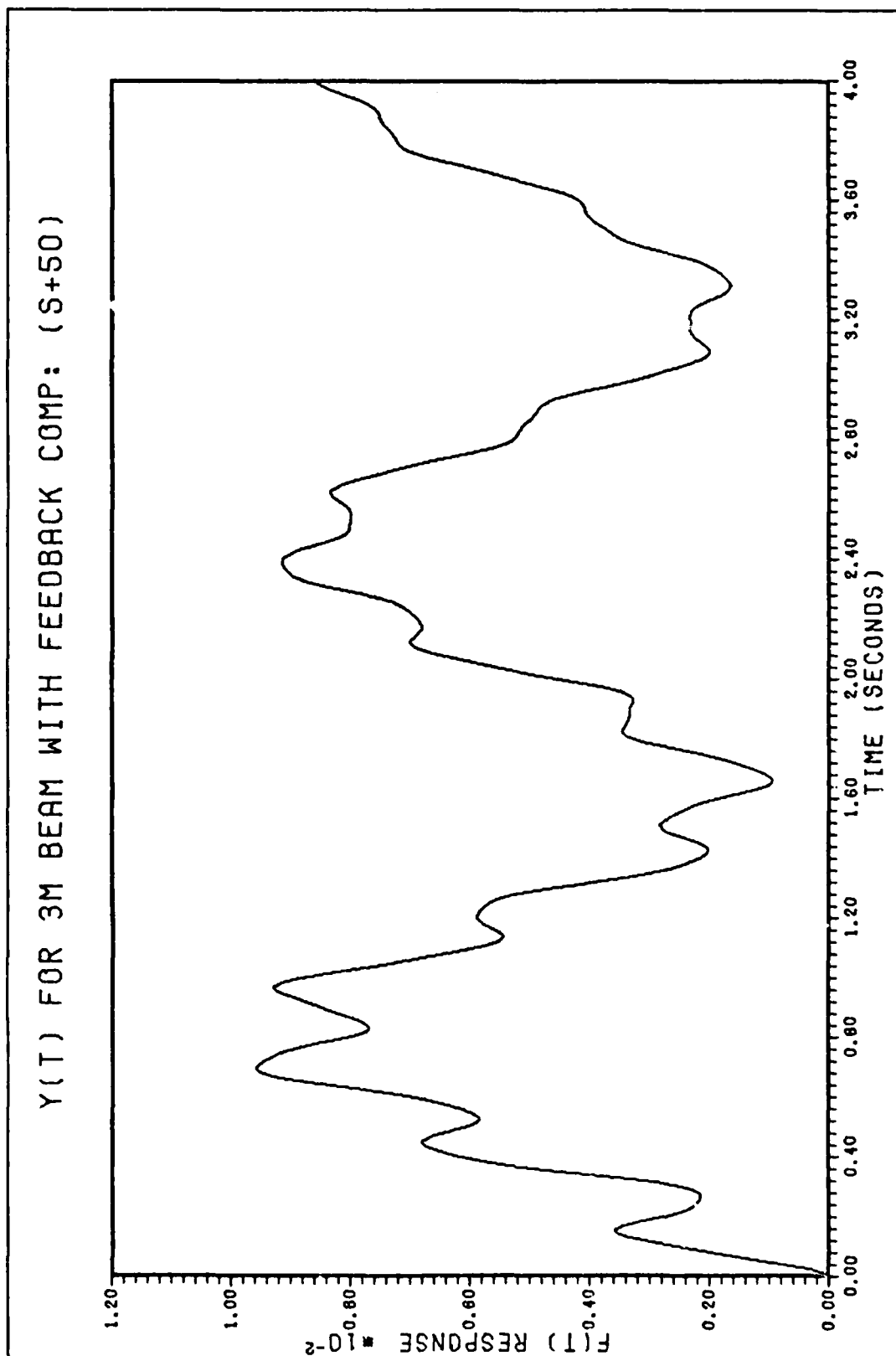
Figure B28. Sensor displacement for one zero at −50.

Y(T) FOR 3M BEAM WITH FEEDBACK COMP: S(S+40)
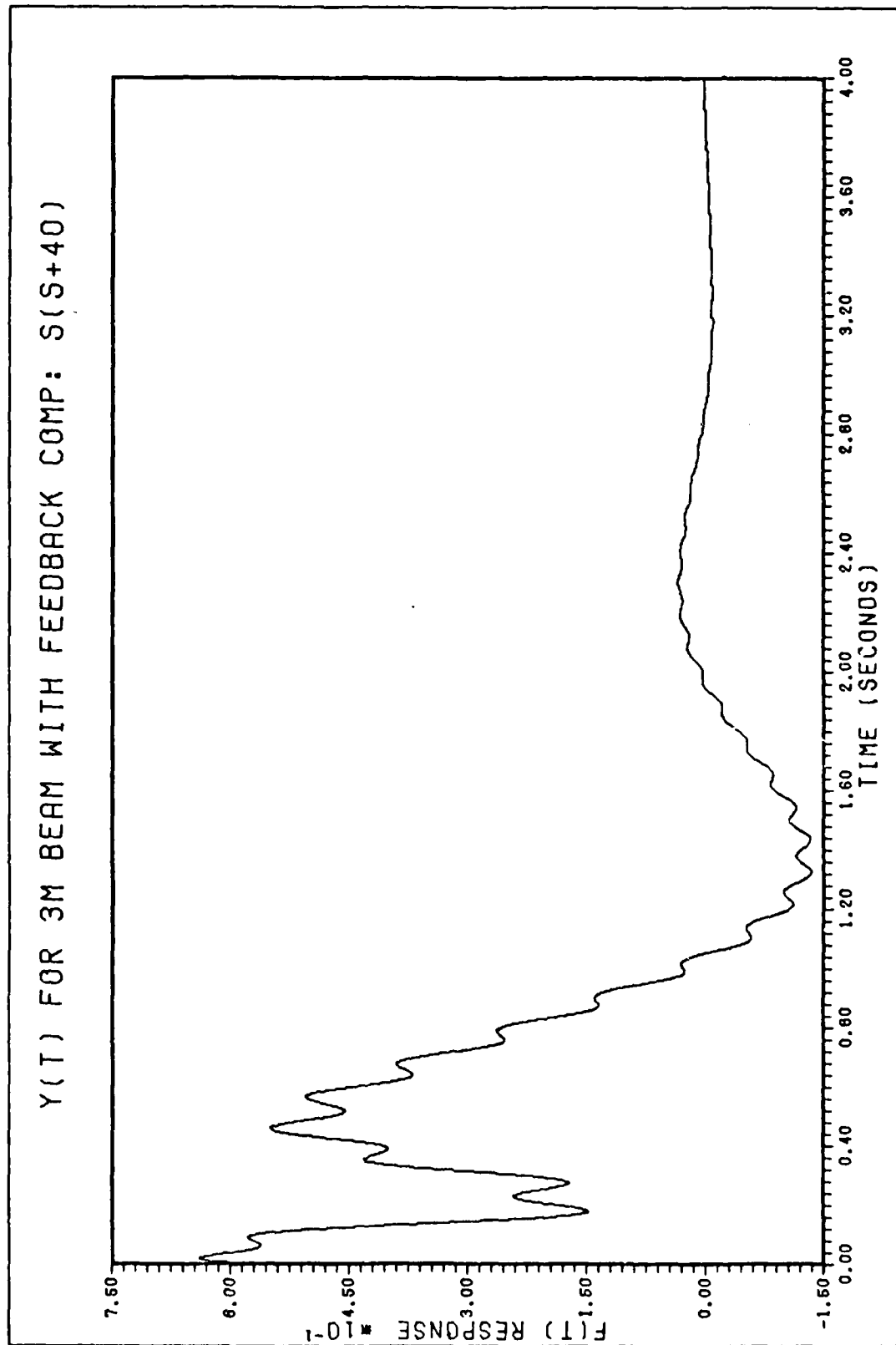
Figure B29. Sensor displacement for zeroes at origin and -40.

Appendix C

Computer Output for Position, Rate, and Position-Rate Sensors

CANTILEVERED BEAM WITH POSITION SENSOR AND LUENBERGER OBSERVER AND 1 RESIDUAL MODE

SENSOR POSITION = .6
ACTUATOR POSITION = .400
BEAM LENGTH = 1.0
BEAM MASS DENSITY/UNIT LENGTH = .394437
BEAM STIFFNESS (EI) = .31025E+02
ROOTS OF CHARACTERISTIC EQUATION:
   FIRST MODE: .19750000000000E+01
   SECOND MODE: .46540000000000E+01
   THIRD MODE: .78560000000000E+01
NATURAL FREQUENCIES:
   FIRST MODE: .31179434385944E+02
   SECOND MODE: .10541259957692E+03
   THIRD MODE: .54721595367042E+03

THE "A" MATRIX

.1000000E+01   0.

0.   .1000000E+01

0.   0.

-.7216025E+03   0.

-.3716300E+03   0.

THE "B" MATRIX, TRANSPOSED

-.7320097E+00   .2176471E+01

0.   0.

THE "C" MATRIX

-.1651915E+01   .1772418E+01   0.

0.

THE "L" MATRIX (RESIDUAL)

0.

THE "B" MATRIX FOR RESIDUALS, TRANSPOSED

0.   .1001909E+01
-.2034653E+00   0.

-.1674464E+01   0.

THE "C" MATRIX FOR RESIDUALS

.1000063E+01   0.

THE "G" MATRIX

THE "G" MATRIX

THE "X" MATRIX, TRANSPOSED

THE "I-KC" MATRIX

THE EIGENVALUES OF I-KC

THE AVERAGE REAL PART =   -.357445043134E+32   DESIRED ROOT =   -.342443564013bE+b2

THE EIGENVALUES OF THE SYSTEM

-78-

THE LEFT SIDE OF THE SYSTEM MATRIX

THE RIGHT SIDE OF THE SYSTEM MATRIX

THE M + PS - KG MATRIX

M + PS - KG EIGENVALUES

CANTILEVERED BEAM WITH VELOCITY SENSOR AND LUENBERGER OBSERVER AND 1 RESIDUAL MODE

SENSOR POSITION   =   .6
ACTUATOR POSITION   =   .400
BEAM LENGTH   =   1.0
BEAM MASS DENSITY/UNIT LENGTH =   .394437
BEAM STIFFNESS (EI) =   .31026E+02
ROOTS OF CHARACTERISTIC EQUATION:
    FIRST MODE: .19750000000000075E+01
    SECOND MODE: .46540000000000005E+01
    THIRD MODE: .78550000000000075E+01
NATURAL FREQUENCIES:
    FIRST MODE: .31179463438534E+02
    SECOND MODE: .19541129057852E+03
    THIRD MODE: .54721595367304E+03

THE "A" MATRIX

0.   .1C00C00E+01   0.   .1C00C00E+01
0.   0.   0.
-.9721602E+C3   -.2418E83E+05   0.
0.

THE "B" MATRIX, TRANSPOSED

0.   -.7320097E+C0   .2176471E+C1

THE "C" MATRIX

0.   -.1C654C1E+C1   .1F77218E+C1

THE "A" MATRIX (RESIDUAL)

.2594453E+06   0.   .1C9C0005+C1
-.

THE "B" MATRIX FOR RESIDUALS, TRANSPOSED

0.   -.1F74E44E+C1

THE "C" MATRIX FOR RESIDUALS

0.   .1E03EF3E+C1

THE "G" MATRIX

THE RICCATI SOLUTION

.2781955+02	.3783264E+03	-.2035430E+02	.2220065E+02	
.2973631E+05	.9521257E+03	-.1409973E+00	.1273475E+02	
.8521257E+03	.4622263E+06	-.5100145E+03	-.1786247E+01	
-.1409973E+00	-.5100049E+03	.3248277E+02	.2389309E+00	
-.1273475E+02	-.1786247E+01	.2389309E+00	.1031741E+02	

THE WEIGHTS USED
500. 500. 500. 500.
FMT = 1.

THE "A+BG" MATRIX

0.	.1000000E+01	0.	
0.	0.	.1000000E+01	
-.8517887E+03	.2703629E+03	-.1636362E+02	.1630965E+02
-.8065631E+02	-.3895137E+05	-.8653665E+02	-.4469320E+02

THE EIGENVALUES OF A+BG

(-8.14360E,334.7,30.632409842740)
(-8.13362E5307,-30.032-30.42749)
(-24.24435640130,193.87947357660)
(-24.24450+0136,-103.47947357784)
THE SMALLEST REAL PART = -.2424456+0136E+02

THE "K" MATRIX, TRANSPOSED

$-.917341E-C1$ $.4375275+CO$ $-.79516575+00$ $.7554281E+02$

THE "A-KC" MATRIX

0.	.8552241E+00	.1722639E+00
0.	.6424657E+30	.1786654E+00
$-.6721637+03$	$-.1103090E+01$	.1994577E+01
0.	.1109271E+03	$-.1418103E+03$
0.	$-.3413603E+05$	

THE EIGENVALUES OF A-KC

$(-34.2443805E+5,0.)$
$(-35.2443505763,0.)$
$(-36.2443505+214,0.)$
$(-37.24455621193,0.)$

THE AVERAGE REAL PART = $-.3574485640135+02$ DESIRED ROOT = $-.3424435640136E+02$

THE EIGENVALUES OF THE SYSTEM

$(-207.3+43945181,645.405315113)$
$(-207.38439551C1,-645.859615113)$
$(3.600253445,07,256.5660119026)$
$(3.600259466517,-205.56601119026)$
$(166.56717019181,0.)$
$(-4.036730305541,31.+466165875624)$
$(-4.036730305541,-31.+465187624)$
$(17.2761451C155,22.0536637375i)$
$(17.2761461165,-22.3536567731)$
$(6.6736233534565,0.)$

THE LEFT SIDE OF THE SYSTEM MATRIX

THE RIGHT SIDE OF THE SYSTEM MATRIX

THE "A + BG - KC" MATRIX

THE "A + BG - KC" EIGENVALUES

(-10.5169...+21E, 59.4021137277E3)
(-10.5169...+21E, -69.4021137277E3)
(-184.45231+5469, 0.)
(-2.35021110-964, 0.)

CANTILEVER BEAM WITH POSITION AND VELOCITY SENSOR AND LUENBERGER OBSERVER AND 1 RESIDUAL MODE

```
SENSOR POSITION =      .5
ACTUATOR POSITION =       .400
BEAM LENGTH =   1.0
BEAM MASS DENSITY/UNIT LENGTH =   .394437
BEAM STIFFNESS (EI) =     .31325E+02
ROOTS OF CHARACTERISTIC EQUATION:
     FIRST MODE:   .18750000000000E+01
     SECOND MODE:  .46940000000000E+01
     THIRD MODE:   .76550000000000E+01
NATURAL FREQUENCIES:
     FIRST MODE:   .31179483,395945E+02
     SECOND MODE:  .19541259057892E+03
     THIRD MODE:   .54721595367304E+03
```

THE "A" MATRIX

0.   0.   .10000000E+01   0.

0.   0.   0.   .10000000E+01

-.37216025+03   -.79186608E+05   0.   0.

0.   0.   0.   0.

THE "B" MATRIX, TRANSPOSED

0.   -.73200375E+00   .21754715E+01

THE "C" MATRIX

-.16634015+01   .19772156+01   -.16554015E+01   .18772158E+01

THE "A" MATRIX (RESIDUAL)

0.   .10000000E+01
-.29344535+05   0.

THE "B" MATRIX FOR RESIDUALS, TRANSPOSED

0.   -.16766405E+01   .15089635E+01

THE "C" MATRIX FOR RESIDUALS

.15059635E+01

-86-

THE "G" MATRIX

THE RICCATI SOLUTION

.27816935+03   .77002644E+03   -.2235473E+02   .22230655E+02

.29756915+05   .57212657E+03   -.1405973E+00   -.1273475E+02

.35212575+03   .40222607+06   -.5108043E+03   -.17357247E+01

-.143697735+05 -.51080495+02   .7124877E+02   .2393703E+00

-.1273475E+02   -.1786247E+01   .2393303E+00   .1031711E+02

THE WEIGHTS USED
500. 500. 500.
FWT = 1.

THE "A+BG" MATRIX

0.   0.   .10000000E+01   0.

0.   0.   0.   .10000000E+01

-.951795E+02   -.7705295E+03   -.1635362E+02   .16703665E+02

-.5055931E+02   -.7790143E+05   .4865765E+02   -.4863320E+02

THE EIGENVALUES OF A+BC

(-8.19355393307, 30.932.7812745)
(-9.19355393307, -30.092.5642776)
(-24.2448564017, 103.8-94735784)
(-24.2448564017, -103.8794735784)
THE SMALLEST REAL PART =   -.24245856601136E+02

THE "C" MATRIX, TRANSPOSED

$-.325073E-01$ $.794943E+00$ $-.703F573E+00$ $.7510332E+02$

THE "A-KC" MATRIX

$-.135337E+00$ $.736576E+00$ $.304151E+00$ $.173557E+00$

$.64357E+00$ $-.750265E+00$ $.645757E+00$ $.17-3734E+00$

$-.373197E+02$ $.172091E+01$ $-.103772E+01$ $.13209193E+01$

$.11023193E+03$ $.363270E+05$ $.112913E+03$ $-.1499533E+03$

THE EIGENVALUES OF A-KC

$(-37.2+.386272E6,0.)$
$(-26.2+43557.4441,0.)$
$(-35.2++3855021 7,9.)$
$(-3..2++35557C2,0.)$

THE AVERAGE REAL PART = $-.3574435401 74E+02$ DESIRED ROOT = $-.342485640135E+02$

THE EIGENVALUES OF THE SYSTEM

$(-207.2093306 00,50.40756530 11)$
$(-207.2093306 00,-50.40756530 11)$
$(3.90204683 02,05.5915C0215)$
$(3.90204683 02,-205.5715905 13)$
$(16.17477374 7A,0.)$
$(-6.05745653 00,71.40706146 15)$
$(-6.05745653 00,-71.40706146 15)$
$(17.1506265 007,54.04291002)$
$(17.1506265 007,-54.04291002)$
$(5.40367+46024,0.)$

-88-

THE LEFT SIDE OF THE SYSTEM MATRIX

THE RIGHT SIDE OF THE SYSTEM MATRIX

THE "A + BG - KC" MATRIX

"A + BG - KC" EIGENVALUES

(-184.05267573745, 0.)
(-19.3+25077707C5, 19.25-594.0519)
(-10.34253737570 5, -69.2-5594050C)
(-3.0785438314w, 0.)

VITA

Donald T. Palac was born April 8, 1955 in Evanston, Illinois. After graduating from high school in 1973 in Dundee, Illinois, he attended Purdue University. While at Purdue he participated in the ROTC program. He graduated from Purdue in May, 1977, and received a Bachelor of Science of Aeronautical Engineering and his commission in the USAF. His active duty career began at the Air Force Institute of Technology in October, 1977.

REPORT DOCUMENTATION PAGE		READ INSTRUCTIONS BEFORE COMPLETING FORM
1. REPORT NUMBER AFIT/GA/AA/78D-6	2. GOVT ACCESSION NO.	3. RECIPIENT'S CATALOG NUMBER
4. TITLE (and Subtitle) ANALYSIS OF ACTIVE CONTROL OF CANTILEVER BEAM BENDING VIBRATIONS		5. TYPE OF REPORT & PERIOD COVERED MS Thesis
		6. PERFORMING ORG. REPORT NUMBER
7. AUTHOR(s) Donald Thomas Palac 2 Lt		8 CONTRACT OR GRANT NUMBER(s)
9. PERFORMING ORGANIZATION NAME AND ADDRESS Air Force Institute of Technology AFIT-EN, Wright Patterson AFB, Ohio 45324		10. PROGRAM ELEMENT, PROJECT, TASK AREA & WORK UNIT NUMBERS
11. CONTROLLING OFFICE NAME AND ADDRESS		12. REPORT DATE December 1978
		13. NUMBER OF PAGES 90
14. MONITORING AGENCY NAME & ADDRESS(if different from Controlling Office)		15. SECURITY CLASS. (of this report) Unclassified
		15a. DECLASSIFICATION/DOWNGRADING SCHEDULE

16. DISTRIBUTION STATEMENT (of this Report)

Approved for public release; distribution unlimited

17. DISTRIBUTION STATEMENT (of the abstract entered in Block 20, if different from Report)

18. SUPPLEMENTARY NOTES

Approved for public release; IAW AFR 190-17

JOSEPH P. HIPPS, Major, USAF
Director of Information

19. KEY WORDS (Continue on reverse side if necessary and identify by block number)

Active modal control
Classical control
Optimal regulator

20. ABSTRACT (Continue on reverse side if necessary and identify by block number)

Active control of bending vibrations in a cantilever beam is examined using a digital computer model of beam and controller. The controller uses the discretized beam equation of motion in a linear control system, which uses a Luenberger observer to reconstruct modal amplitudes and velocities from the sensor output. Feedback gains obtained from a steady state optimal regulator drive a force actuator. The model is used to examine

three areas of active control of bending vibrations. First,
impact on control effectiveness is investigated for iterative
changes in elements of the state weighting matrix, part of the
quadratic performance index minimized for the steady state
optimal regulator. Second, the steady state optimal regulator
is replaced with classical control through addition of open
loop zeroes to the system transfer function. Third, the sensor
model is changed to include position and rate information and
rate information only. State weighting matrix element changes
selectively produce increased damping of the mode associated
with the changed element. Breakdown of the observer model, and
instability, occurs when the change in an element exceeds a
limit peculiar to that element and its relative magnitude.
Control through classical feedback compensation is at least
as effective as optimal control by the steady state optimal
regulator. Addition of rate information to the sensor model
causes instability because of numerical inaccuracies in the
solution of the linear equation producing the Luenberger
observer state estimation.